IN-34
31434
49P

NASA Technical Memorandum 106770
ICOMP–94–26

On the Behavior of Three-Dimensional Wave Packets in Viscously Spreading Mixing Layers

Thomas F. Balsa
Institute for Computational Mechanics in Propulsion
Lewis Research Center
Cleveland, Ohio

and University of Arizona
Tucson, Arizona

(NASA-TM-106770) ON THE BEHAVIOR OF THREE-DIMENSIONAL WAVE PACKETS IN VISCOUSLY SPREADING MIXING LAYERS (NASA. Lewis Research Center) 49 p

N95-15908

Unclas

G3/34 0031434

November 1994

National Aeronautics and
Space Administration

INSTITUTE FOR COMPUTATIONAL MECHANICS IN PROPULSION
NASA
ICOMP
Lewis Research Center
Ohio Aerospace Institute

On the Behavior of Three-Dimensional Wave Packets in Viscously Spreading Mixing Layers

Thomas F. Balsa
Institute for Computational Mechanics in Propulsion
Lewis Research Center
Cleveland, Ohio 44135

and University of Arizona
Department of Aerospace and Mechanical Engineering
Tucson, Arizona 85721

We consider analytically the evolution of a three-dimensional wave packet generated by an impulsive source in a mixing layer. The base flow is assumed to be spreading due to viscous diffusion. The analysis is restricted to small disturbances (linearized theory). A suitable high-frequency ansatz is used to describe the packet; the key elements of this description are a complex phase and a wave action density. It is found that the product of this density and an infinitesimal material volume convecting at the local group velocity is *not* conserved: there is a continuous interaction between the base flow and the wave action. This interaction is determined by suitable mode-weighted averages of the second and fourth derivatives of the base-flow velocity profile. Although there is some tendency for the dominant wavenumber in the packet to shift from the most unstable value toward the neutral value, this shift is quite moderate. In practice, wave packets do not become locally neutral in a diverging base flow (as do instability modes), therefore, they are expected to grow more suddenly than pure instability modes and do not develop critical layers. The group velocity is complex; the full significance of this is realized by analytically continuing the equations for the phase and wave action into a complex domain. The implications of this analytic continuation are discussed vis-a-vis the secondary instabilities of the packet: very small-scale perturbations on the phase can grow very rapidly initially, but saturate later because most of the energy in these perturbations is convected away by the group velocity. This remark, as well as the one regarding critical layers, has consequences for the nonlinear theories.

1. Introduction

An unstable shear flow, when excited by an external disturbance that is compact in space and impulsive in time, is capable of *dispersing* this concentrated disturbance into a wave train (or wave packet) of finite extent, which is convected by the underlying (unstable) base flow. The classical work is due to Gaster (1975; Gaster & Grant 1975). The term dispersion is used here in a generalized sense: not only do the various Fourier components of the initial disturbance travel at different phase speeds (resulting in a broadening of the spatial extent of the disturbance at subsequent instants of time), but they also possess different growth rates. Therefore, any concentrated disturbance in the flow evolves into a wave packet owing to the 'slippage' of the various Fourier components with respect to each other *and* to the changes in the relative magnitudes of these components, because of their different growth rates.

It is fair to say that our theoretical understanding of how such a wave packet evolves in a homogeneous parallel base flow, under the small disturbance approximation (i.e. linearized analysis), is quite complete (Criminale & Kovasznay 1962; Tam 1967; Gaster 1975; Balsa 1988, 1989a). This is because we may use Fourier-Laplace transforms in (x - z) space and time (see figure 1) to solve the initial value problem and then evaluate the corresponding inverse transforms, for large values of time, by standard asymptotic methods. This yields a concise mathematical description of a wave packet, including its receptivity with respect to the disturbance-producing impulse (Balsa 1989a).

On the other hand, when the underlying base flow is inhomogeneous, either in space or time, Fourier-Laplace methods are no longer applicable. If the inhomogeneity is weak in the sense that the base flow changes slightly over one wavelength of the primary oscillation in the packet, a suitable high-frequency analysis may be used (Balsa 1989b). Before we continue our discussion of this analysis, it is necessary to recall that our wave packet has a modal structure (in the y-direction) and the above-mentioned

Fourier components are associated with (x, z)-space; the convection and dispersion of the packet also occur in this space. Therefore, any weak inhomogeneity of the base flow is understood to be in (x, z)-space and possibly in time, and the dependence of the base flow on the cross-space variable, y, is arbitrary (see figure 1). Finally, we emphasize that our attention is focused on wave packets generated by spatially compact and temporally impulsive disturbances; it is possible to generate wave packets (or, precisely, modulated wave trains) of much longer spatial extent by slowly varying the amplitude or frequency of a spatial instability mode that is excited by a wave-maker. We plan to examine the properties of these modulated wave trains in a forthcoming paper.

The evolution of spatial instability modes in slightly inhomogeneous base flows has been examined by a number of authors; perhaps the most relevant work for our purposes is that of Crighton & Gaster (1976). These investigators found that as the mode propagates downstream in a slowly diverging jet flow, the instability becomes weaker and, as a result, the amplitude of the mode grows at a diminishing rate. In fact, there is a streamwise location at which the spatial instability mode is locally neutral and, at this location, the modal amplitude levels off. In other words, the instability wave saturates because of flow divergence. Although these observations are helpful in the interpretation of certain experimental data (e.g. Gaster, Kit & Wygnanski 1985), Goldstein & Leib (1988) recognized a very different significance, which provided the framework for the rational composite description of the *nonlinear* evolution of an instability mode.

Goldstein & Leib (1988; see also Hultgren 1992) argued that the evolution of an instability mode in a diverging base flow merely represented the disturbed flow in a suitable outer (i.e. upstream) region. This outer region slowly drives the most unstable mode (generated at some location, say, $x = -\infty$) toward its neutral state; just prior to the attainment of this state, the disturbance develops a distinct critical layer (Maslowe

1981). The flow in this layer is dominated by nonlinear effects, hence the outer region provides the 'initial' conditions for this nonlinear flow analyzed by Goldstein & Leib (1988) using asymptotic methods.

In a broad sense, our original objectives in embarking on this research were twofold: first, the generalization of the ideas of Crighton and Gaster in describing the behavior of three-dimensional instability wave packets evolving on top of slightly inhomogeneous base flows and, second, the application of critical layer concepts, in the spirit of M. E. Goldstein and his colleagues, toward a description of the nonlinear phenomena in these packets. The present paper deals with the first of these objectives in considerable detail, focusing on physical and mathematical issues relating to the possible development of critical layers, the role of the complex group velocity and wave action, and the secondary instabilities of the wave packet owing to the presence of an inhomogeneous base flow. Several novel effects arise in this study—these have important implications for the linear and nonlinear development of wave packets.

There are many approaches to studying the evolution of rapidly varying disturbances (i.e. the wave packet) on a slowly varying system (i.e. the base flow). If the disturbance is periodic, the 'method of averaging' yields the equations on the long scales; when this procedure is applied to the perturbation Lagrangian, a very powerful method results for the description of the disturbance on the slow scales (Whitham 1974; Hayes 1970). Although this method has been used for instability waves, it is only applicable when the growth rates are asymptotically small (Landahl 1982).

For instability waves with finite (but numerically small) growth rates, a high-frequency ansatz, in terms of complex amplitude and phase, is the proper way to proceed (Itoh 1981; Balsa 1989b). One major difference between the analyses in these two references is that the latter introduces the concept of a complex modal wave action, $\mathcal{A}$, which is the product of the square of the amplitude and suitable mode-shapes integrated over cross-space. The importance of the wave action is clear from the classical theories for conservative wave systems.

The present paper continues from where Balsa (1989b) left off. The outline is as follows: In §2 the problem is formulated, the base-flow and disturbance equations are briefly discussed, and the equations for the phase and the wave action are provided for reference so that the reader does not have to consult Balsa (1989b), except for details. Section 3 deals with the description of a self-similar base flow and the replacement of a spatially diverging base flow by a temporally spreading flow. We believe that this replacement, which offers a number of technical advantages leading to closed-form solutions, is a very good approximation. A more complete justification is provided later. In §§4 and 5, results are given for the phase and the wave action. The phase, which obeys a canonical dispersion relation because of a Squire-like transformation, involves an integral of the local thickness of the mixing layer; this integral accounts for history (or age) effects as the wave packet travels downstream, encountering sections of a mixing layer whose thickness is slowly increasing. In §5 we provide a simple expression for the complex group velocity, show that its divergence is real, and recast the equation for the wave action into a form, (26*b*), that is most suitable for the discussion that follows in §6. The important physical and mathematical results are discussed in several sub-sections of §6; here attention is called to analytic continuation (near the end of §6.2) and to the secondary instabilities in §6.3.

2. Formulation of the problem

In order to provide some feel for the key equations that will be used in subsequent sections, we rely heavily on the general literature on the evolution of instability waves in slightly inhomogeneous base flows (see Balsa 1989b and references cited therein) and on classical kinematic wave theory (Whitham 1974) and its variants for modal waves (Hayes 1970). Of course, with respect to the latter remark, our formalism is necessarily very different from what is used in the classical theories because the concept of an 'average Lagrangian' cannot be used for instability waves. Generally, these waves are not periodic in space (or time), except when their growth rates are vanishingly small.

2.1. *General remarks*

For the unperturbed base flow, consider an incompressible free-shear flow (such as a laminar mixing layer) whose velocity and pressure are denoted by $\mathbf{U}_\mathrm{B}$ and $p_\mathrm{B} \cong$ const., respectively. At moderately large Reynolds numbers, this flow is approximately "parallel" in the sense that

$$\mathbf{U}_\mathrm{B} = [1 + O(\epsilon^2)]\mathbf{U}(y, \boldsymbol{\xi}, \tau) + \epsilon[1 + O(\epsilon^2)]V(y, \boldsymbol{\xi}, \tau)\mathbf{e}_2 \qquad (1a)$$

$$p_\mathrm{B} = \text{const.} + O(\epsilon^2)\,, \qquad \epsilon << 1 \qquad (1b)$$

where ($\mathbf{e}_1$, $\mathbf{e}_2$, $\mathbf{e}_3$) are the unit vectors along the (x, y, z) directions, respectively; $\mathbf{U} \cdot \mathbf{e}_2 = 0$ (in other words, $\epsilon V << 1$ is the y-component of $\mathbf{U}_\mathrm{B}$ at lowest order). We now proceed to introduce the terminology and notation; the geometry is illustrated in figure 1.

Assume that all variables are nondimensional. Let L_ref and U_ref stand for reference quantities that are used to normalize all lengths and velocities, respectively; we choose L_ref to be the characteristic *thickness* and U_ref to be the characteristic speed of the mixing layer. Thus, the Cartesian coordinate $\mathbf{x} = (x, y, z)$ is nondimensionalized by L_ref, and time, denoted by t, is normalized by the transit time $(L_\mathrm{ref}/U_\mathrm{ref})$. As customary in incompressible flows, pressures are measured in terms of ρU_ref^2, where $\rho =$ const. is the density of the fluid.

The slow spatio-temporal variables used in (1a) are defined by

$$\boldsymbol{\xi} = \epsilon(x\mathbf{e}_1 + z\mathbf{e}_3)\,, \qquad \tau = \epsilon t \qquad (1c)$$

where $\epsilon = (Re)^{-1}$ is a small parameter. Here, $Re =$ const. denotes the Reynolds number of the base flow: $Re = L_\mathrm{ref}U_\mathrm{ref}/\nu >> 1$ ($\nu =$ kinematic viscosity of fluid). Note that this Reynolds number is based on a length scale associated with the *thickness* of the mixing layer rather than on a typical streamwise length scale. For this reason, the expansion of the base flow proceeds in powers of $\epsilon = (Re)^{-1} << 1$ rather than in those of $(Re)^{-1/2}$.

It is well known that, under the stated assumptions, the horizontal component of the fluid velocity at lowest order, $\mathbf{U}$, obeys the boundary layer equations

$$\frac{\mathrm{D}\mathbf{U}}{\mathrm{D}t} = \epsilon \frac{\partial^2 \mathbf{U}}{\partial y^2} \tag{2a}$$

where the time differentiation, following the base flow, is defined by

$$\frac{\mathrm{D}}{\mathrm{D}t} = \frac{\partial}{\partial t} + \mathbf{U}_{\mathrm{B}} \cdot \frac{\partial}{\partial \mathbf{x}} \tag{2b}$$

while the physical law of mass conservation requires

$$\frac{\partial}{\partial \mathbf{x}} \cdot \mathbf{U}_{\mathrm{B}} = 0 \tag{2c}$$

The slow variation of the base flow in the streamwise direction is contained in the fact that (U, V) depend on (x, z, t) through the (slow) variables ξ and τ only. Thus, $\mathrm{DU}/\mathrm{D}t$ is actually of $O(\epsilon)$; therefore, a nontrivial balance is attained in (2*a*) at lowest order. In other words, the slow streamwise evolution of the base flow, arising from its small acceleration (positive or negative), is caused by viscous diffusion.

Let us now assume that this base flow is perturbed by an arbitrary disturbance whose (perturbation) velocity and pressure fields are denoted by $\mathbf{u} = \mathbf{u}(\mathbf{x}, t)$ and $p = p(\mathbf{x}, \mathrm{t})$, respectively. The relevant linearized equations for these quantities are

$$\text{Momentum:} \quad \frac{\mathrm{D}\mathbf{u}}{\mathrm{D}t} + \mathbf{u} \cdot \frac{\partial \mathbf{U}_{\mathrm{B}}}{\partial \mathbf{x}} = -\frac{\partial p}{\partial \mathbf{x}} + \epsilon \nabla^2 \mathbf{u} \tag{3a}$$

$$\text{Continuity:} \quad \frac{\partial}{\partial \mathbf{x}} \cdot \mathbf{u} = 0 \tag{3b}$$

where ∇^2 denotes the Laplacian operator in the variables (x, y, z). Our interest is in the case where the perturbations are the instability waves of the base flow; these waves may be considered inviscid when the Reynolds number of the base flow is larger than about 500 (Betchov & Szewczyk 1963) and the base-flow profile possesses an inflection point. Therefore, we ignore the last term in (3*a*) and assume that, in principle, $\mathbf{U}_{\mathrm{B}}$ is a known function of its arguments.

The following remarks should reassure the reader that the neglect of the viscous terms in (3*a*) does not vitiate any of the major conclusions of this paper. First note that viscous effects show up in (2*a*) and (3*a*); these, respectively, produce a viscously spreading mixing layer and a (locally) small correction to the inviscid instability modes of this layer. However, over the long (or global) streamwise scale of interest, namely $x = O(Re) = O(\epsilon^{-1})$, both of these viscous effects formally produce an order-one correction to the disturbance.

On the other hand, it is well known from the classical theories of wave motion that slight inhomogeneities in a base flow can produce important and subtle effects (e.g. a complex group velocity in our case) on the wave-like disturbances sustained by this flow. It is precisely some of these new physical effects that we wish to uncover in this paper.

To put it more quantitatively, suppose we replace ϵ in (3*a*) by $(\Gamma\epsilon)$, where (for the purposes of the asymptotics) $\Gamma = O(1)$. Now we have essentially tagged the viscous correction to the instability modes via the parameter Γ (which, of course, ultimately must be set to unity), and separated this correction from the effects of a spreading base flow. The latter effects show up as variable coefficients in (3*a*). When this is done, it is found that the coefficient, H, in (10*a*) contains an extra term arising from the viscous term in (3*a*) (see Balsa 1994; Hultgren 1992). Hence, H contains *additively* the effects of base-flow inhomogeneity and those of viscosity. Therefore, it should be remembered that the remarks we later direct at H apply only to the effects of a nonuniform base flow.

To summarize, our objective is to provide a family of inviscid solutions for (3) when the base flow varies slowly in the streamwise and spanwise coordinates (x, z), and time t, owing to the viscous diffusion of this flow.

2.2. *Fluid displacement*

The so-called primitive variables for the incompressible equations of fluid mechanics are the velocity and pressure. These variables are convenient to use in a large class of small-disturbance problems, especially when the base flow is a uniform stream. On the other hand, when the base flow is dependent on space or time, even if this dependence is slow in some sense, the use of these primitive variables is not convenient for wave-like problems. This is because, often, there is a subtle energy exchange between the base flow and the wave.

Classically, it is well known that for waves that do not exhibit an exponential growth or decay, a most powerful technique for capturing this energy exchange is via a variational principle and Whitham's (1974) average Lagrangian, which arises from this principle. This suggests that the proper dependent variables to use for instability waves traveling on an inhomogeneous base flow are those in which the equations of motions may be expressed in terms of a simple variational principle. These dependent variables are the fluid particle displacement and pressure; for a disturbance about a known base flow, the perturbation displacement is clearly the most useful. In addition, it is simplest to consider this displacement as a function of $\mathbf{x}$ and t rather than that of a Lagrangian (i.e. particle) label and time. This leads to a hybrid Eulerian-Lagrangian description for the instability wave, which is especially simple for linearized problems (Andrews & McIntyre 1978).

Therefore, in order to provide the disturbance equations in their purest form, we replace the disturbance velocity $\mathbf{u}$ by a displacement variable $\boldsymbol{\alpha} = \boldsymbol{\alpha}(\mathbf{x}, t)$ such that

$$\mathbf{u} = \frac{D\boldsymbol{\alpha}}{Dt} - \boldsymbol{\alpha} \cdot \frac{\partial \mathbf{U}_B}{\partial \mathbf{x}} \tag{4}$$

A physical interpretation for $\boldsymbol{\alpha} = \boldsymbol{\alpha}(\mathbf{x}, t)$ is this: Consider a fluid particle of fixed identity that occupies the point $\mathbf{x}$ (at time t) in the unperturbed base flow. The position of this same particle in the perturbed flow (at time t) is defined to be $(\mathbf{x} + \boldsymbol{\alpha})$. In other words, the particle that would have been at $\mathbf{x}$ in the base flow is actually in a slightly different position (namely, $\mathbf{x} + \boldsymbol{\alpha}$) in the disturbed flow.

Before we provide an asymptotic solution of (3) using a high-frequency ansatz, it is useful to introduce some terminology. First, we think of the y-direction as the *cross-space* (in which our disturbance has a mode-like structure) and of the ξ-space as *propagation space* (in which our disturbance has a wave-like structure). Second, the entire effect of base-flow spreading is succinctly contained in $\mathcal{F}$ (Balsa 1989b), where

$$\mathcal{F} = \frac{\partial^2 \mathbf{U}}{\partial y^2} \tag{5}$$

Finally, note that $\mathcal{F}$ lies in propagation space and represents the (nondimensional) force acting on a unit volume of fluid in the boundary-layer approximation.

2.3. *High-frequency ansatz*

The basic variables that we use to characterize a disturbance are the displacement and perturbation pressure, $(\boldsymbol{\alpha}, p)$. We expand these (see Balsa 1989b for details) according to the usual high-frequency ansatz

$$\boldsymbol{\alpha} = \boldsymbol{\alpha}(\mathbf{x}, t) = (\boldsymbol{\alpha}^{(0)} + \epsilon\boldsymbol{\alpha}^{(1)} + \ldots) \exp(i\phi/\epsilon) + \mathrm{cc} \tag{6}$$

where $i = \sqrt{-1}$ and cc stands for the complex conjugate of the term immediately preceding it. A similar expansion holds for p; $\phi = \phi(\xi, \tau)$ is the complex phase of the disturbance and $\boldsymbol{\alpha}^{(j)} = \boldsymbol{\alpha}^{(j)}(y, \xi, \tau)$ for $j = 0, 1$. We emphasize that ϕ is complex, although usually we refer to it simply as the phase.

The physical picture is that the base flow evolves on a 'long or slow' spatio-temporal scale that is proportional to the Reynolds number while the *local* behavior of the disturbance is determined by 'short or fast' spatio-temporal scales characterized by the shear layer thickness and associated convection times. On the other hand, the *global* evolution of the disturbance is dictated by the slow scales; hence the relevance of a high-frequency ansatz.

After substituting (4,6) into the linearized disturbance equations (3), and requiring a non-trivial solution for $(\cdot)^{(0)}$, we find the evolution equation for the phase

$$-\frac{\partial \phi}{\partial \tau} = \Omega(\nabla\phi, \boldsymbol{\xi}, \tau) \tag{7a}$$

where $\Omega = \Omega(\mathbf{k}, \boldsymbol{\xi}, \tau)$ is, in principle, a *known* function of its arguments expressing the complex local frequency, $\omega = \Omega = -\partial\phi/\partial\tau$, as a function of the complex local wave vector, $\mathbf{k} = \nabla\phi$. We call Ω the dispersion relation, and much of stability theory deals with the determination of Ω for a variety of flows (Drazin & Reid 1981). More generally, a dispersion relation is of the form $\mathscr{D}(\partial\phi/\partial\tau, \nabla\phi, \boldsymbol{\xi}, \tau) = 0$; in using (7*a*), we have assumed that $\mathscr{D} = 0$ may be solved explicitly for $\partial\phi/\partial\tau$. For an incompressible mixing layer, there is one such solution that represents the unstable mode of interest.

Note that ∇ is the gradient operator in propagation space ($\partial/\partial\mathbf{x}$ was used for this operator in physical space) defined by

$$\nabla = \mathbf{e}_1 \frac{\partial}{\partial \xi} + \mathbf{e}_3 \frac{\partial}{\partial \zeta} \tag{7b}$$

where $\boldsymbol{\xi} = (\xi, \zeta) = \xi\mathbf{e}_1 + \zeta\mathbf{e}_3$. Both the frequency and wave vector, $(\omega, \mathbf{k})$, are local in the sense that they depend on $\boldsymbol{\xi}$ and τ due to the viscous spreading of the base flow.

Furthermore, having satisfied the dispersion relation via (7*a*), the lowest-order solutions $(\boldsymbol{\alpha}^{(0)}, p^{(0)})$ must be proportional to an instability mode that can be supported by the base flow. If $p_{\mathrm{m}} = p_{\mathrm{m}}(y, \boldsymbol{\xi}, \tau, \mathbf{k})$ is the pressure mode at wave vector $\mathbf{k}$ and ω_0 is the Doppler-shifted frequency defined by

$$\omega_0 = \omega_0(y, \boldsymbol{\xi}, \tau) = -\left[\frac{\partial \phi}{\partial \tau} + \mathbf{U}\cdot\nabla\phi\right] \tag{8a}$$

then the lowest-order solution is given by

$$p^{(0)} = A(\boldsymbol{\xi}, \tau)p_{\mathrm{m}}(y, \boldsymbol{\xi}, \tau, \nabla\phi) \tag{8b}$$

where $A = A(\boldsymbol{\xi}, \tau)$ is the slowly varying complex amplitude of the disturbance. Similarly,

$$\boldsymbol{\alpha}^{(0)} = A(\xi, \tau)(Q\mathbf{e}_2 - i\mathbf{W}), \qquad \mathbf{W} \cdot \mathbf{e}_2 = 0 \tag{9a}$$

where

$$Q = Q(y, \xi, \tau) = \frac{1}{\omega_0^2} \frac{\partial p_m}{\partial y} \tag{9b}$$

$$\mathbf{W} = \mathbf{W}(y, \xi, \tau) = -\frac{\nabla\phi}{\omega_0^2} p_m \tag{9c}$$

and p_m on the right-hand sides of (9*b*,*c*) is to be evaluated at $\mathbf{k} = \nabla\phi$.

Two remarks are in order: First $p_m = p_m(y, \xi, \tau, \mathbf{k})$ satisfies a Rayleigh-like instability equation at wave vector $\mathbf{k}$; the coefficients of this equation depend parametrically on ξ and τ owing to the inhomogeneity of the base flow. Second, the separation of the displacement $\boldsymbol{\alpha}^{(0)}$ (or more precisely the displacement mode) into components in cross- and propagation spaces (in terms of Q and $\mathbf{W}$) is done for convenience (see (10b)).

In order to solve for the $(\cdot)^{(1)}$ perturbations, a solvability condition must be satisfied. This condition determines the evolution of the amplitude $A(\xi, \tau)$ or, more properly, the evolution equation of the complex wave action density, $\mathcal{A} = \mathcal{A}(\xi, \tau)$, on the long scales

$$\frac{\partial \mathcal{A}}{\partial \tau} + \nabla \cdot (\mathbf{G}\mathcal{A}) + H\mathcal{A} = 0 \tag{10a}$$

where

$$\mathcal{A} = \mathcal{A}(\xi, \tau) = A^2 \int_{-\infty}^{\infty} \omega_0 (Q^2 + \mathbf{W} \cdot \mathbf{W}) dy \tag{10b}$$

and

$$H = \frac{\displaystyle\int_{-\infty}^{\infty} Q \frac{\partial \mathcal{F}}{\partial y} \cdot \mathbf{W} dy}{\displaystyle\int_{-\infty}^{\infty} \omega_0 (Q^2 + \mathbf{W} \cdot \mathbf{W}) dy} \tag{10c}$$

Recall that $\mathcal{F}$ is defined by (5) and note that H accounts for the viscously spreading base flow interacting with the inviscid wave packet. It is precisely this factor that vanishes in classical kinematic wave theory--thereby (10a) reduces to a conservation equation for the wave action density $\mathcal{A}$. The complex group velocity, $\mathbf{G}$, is defined by

$$\mathbf{G} = \left.\frac{\partial\Omega(\mathbf{k}, \xi, \tau)}{\partial\mathbf{k}}\right|_{\mathbf{k} = \nabla\phi} \tag{11}$$

so that ultimately both $\mathbf{G}$ and H (both complex) depend on ξ and τ only. Thus (10a) is a partial differential equation for $\mathcal{A}$ in propagation space and time; this equation, together with that for the phase, (7a), provides the lowest-order uniformly valid solutions for the disturbances on the long spatio-temporal scales. In a linear theory, (7a) and (10a) are effectively uncoupled.

The rest of this paper is devoted to obtaining solutions to these equations under reasonable physical and mathematical assumptions, and to examining the secondary instabilities of these solutions. We remind the reader that a detailed derivation of the previously mentioned evolution equations for ϕ and $\mathcal{A}$ may be found in Balsa (1989b).

3. Temporally spreading base flow

Although the mathematical problems for the base flow and the disturbance may be formulated quite concisely and with total generality (as in §2), the solutions to these general problems are completely numerical. What we want to accomplish in this study is to gain a thorough qualitative understanding of the physics and to generate semi-quantitative results for a three-dimensional wave packet evolving in a spreading base flow, such as a mixing layer. Therefore, we shall make a number of additional approximations. These will enable us to obtain representative and illuminating closed-form results.

A wave packet is a wave train of finite extent; because of the instability of the base flow and the resultant exponential growth of the disturbance, the dominant part of a packet consists of a few oscillations only (Gaster 1975; Balsa 1989a). Thus the overall length of a wave packet is very much smaller than the long viscous scales on which the base flow is evolving, therefore at each instant of time, the spatial spreading or divergence of the mixing layer is unimportant. Of importance is that at two instants of time, say, τ_1 and τ_2, the wave packet is at successive streamwise locations, say, ξ_1 and ξ_2, at which the thicknesses of the mixing layer may be very different. It is possible to simulate this effect by allowing the thickness to depend on time rather than space. This approximation is equivalent to a temporally spreading base flow whose characteristic thickness is $\delta = \delta(\tau)$.

With this approximation at hand, we write

$$\mathbf{U} = U(y, \tau)\mathbf{e}_1 \ , \qquad V = 0 \tag{12a}$$

so that the base flow is parallel to the x-axis. U obeys the classical diffusion equation (to which (2*a*) reduces under the stated assumptions), for which we can obtain a class of closed-form solutions. For example, if the two external streams of the mixing layer are brought into contact at some early time, say, $\tau = -1$, the vortex sheet between these streams quickly diffuses into a mixing layer of finite thickness and U is expressible in terms of the error function whose argument is the similarity variable

$$\eta = \frac{y}{\delta(\tau)} \tag{12b}$$

where

$$\delta = \delta(\tau) = (1 + \tau)^{1/2} \tag{12c}$$

In view of these preliminary remarks, we write

$$U = U(\eta) \tag{13}$$

where U on the right-hand side of (13) is any reasonable function (e.g. error, tanh, etc.)

that approximates the velocity profile of a mixing layer and $\delta(\tau)$ is more or less an arbitrary monotonically increasing function of time; $\delta(0) = 1$. We include this generalization over (12*c*) in order to estimate the robustness of our physical model, although most of our discussion (unless otherwise stated) will invoke (12*c*) in order to represent the effects of molecular diffusion most realistically. However, for 'turbulent' diffusion it is much more reasonable to set $\delta(\tau) = 1 + \tau$ (Gaster *et al.* 1985).

We are now in a position to provide a more complete picture of the generation of the wave packet. Suppose our base flow is perturbed at $\tau = 0$ (when $\delta = 1$) by a spatially compact disturbance that is impulsive in time. The concentrated disturbance imparted to the flow quickly disperses into a wave train of finite extent, which contains the exponentially growing part of the disturbance signal, arising from the instability of the mixing layer. The entire wave train is convected downstream (at a convection speed, say, U_c) while the disturbance at the center of the packet is growing at the maximum growth rate associated with temporal instability. The formation and evolution of such a wave packet is well understood in the case of a non-spreading flow (i.e. $\delta \equiv 1$); our objective is to describe this evolution in a self-similarly spreading base flow (i.e. $\delta = \delta(\tau)$).

4. Dispersion relation and the phase

Under the assumption that the base-flow velocity profile depends only on the similarity variable $\eta = y/\delta(\tau)$, considerable progress can be made in representing the dispersion relation and the modes in terms of certain canonical quantities. Let us consider a function $P = P(\eta)$ (the canonical pressure) that satisfies a Rayleigh-like equation

$$[C - U(\eta)]^2 \frac{\partial}{\partial \eta}\left[\frac{1}{[C - U(\eta)]^2} \frac{\partial P}{\partial \eta}\right] - \kappa^2 P = 0 \qquad (14a)$$

with boundary conditions $P \to 0$ as $\eta \to \pm\infty$. Here, κ is a given complex number. In order to obtain a nontrivial solution to (14a) we must have

$$C = C(\kappa) \tag{14b}$$

and

$$P = P(\eta, \kappa) \tag{14c}$$

On the other hand, the actual pressure mode, $p_m = p_m(y, \tau, \mathbf{k})$, satisfies the Rayleigh instability equation

$$[\Omega - kU(\eta)]^2 \frac{\partial}{\partial y}\left[\frac{1}{[\Omega - kU(\eta)]^2} \frac{\partial p_m}{\partial y}\right] - \mathbf{k} \cdot \mathbf{k}\, p_m = 0 \tag{15}$$

where the wave vector is $\mathbf{k} = (k, \ell) = k\mathbf{e}_1 + \ell\mathbf{e}_3$ and the dispersion relation is $\Omega = \Omega(\mathbf{k}, \tau)$. The boundary condition requires that $p_m \to 0$ as $y \to \pm\infty$.

Upon recalling that $\eta = y/\delta(\tau)$ and comparing (14) and (15), we find

$$p_m(y, \tau, \mathbf{k}) = P[\eta, \delta(\tau)\,(k^2 + \ell^2)^{1/2}] \tag{16a}$$

$$\frac{\Omega(\mathbf{k}, \tau)}{k} = C[\delta(\tau)\,(k^2 + \ell^2)^{1/2}] \tag{16b}$$

where $\mathbf{k} \cdot \mathbf{k} = k^2 + \ell^2$. In some sense, (16$a,b$) may be thought of as a Squire-like transformation; more precisely, these equations express the fact that the pressure mode and the complex phase speed, Ω/k, depend on the combined entity $(k^2 + \ell^2)^{1/2}$ rather than individually on k and ℓ.

In view of these remarks, it is easy to see that the canonical quantities P and C represent the pressure and complex phase speed of a two-dimensional mode (at complex streamwise wavenumber $\kappa = k$) at the initial instant of time (when $\delta = 1$). There remains to say a few words about the velocity profile, $U = U(\eta)$, and the canonical phase speed, $C = C(\kappa)$. We set

$$U(\eta) = U_c + \frac{\Delta U}{2} f(\eta) \tag{17a}$$

where

$$U_c = \frac{U_1 + U_2}{2} \tag{17b}$$

$$\Delta U = U_1 - U_2 > 0 \tag{17c}$$

and $f(\eta) \to \pm 1$ as $\eta \to \pm\infty$. Clearly, the speeds in the two external streams of the mixing layer are given by U_1 (= 1) and $U_2 > 0$; see figure 1.

In order to obtain quantitative results, we let

$$f(\eta) = \begin{cases} \tanh \eta & (18a) \\ \text{or} & -\infty < \eta < \infty \\ \operatorname{erf}(\eta) & (18b) \end{cases}$$

These velocity profiles are plotted in figure 2; also shown in this figure are the two-dimensional growth rates of temporal instability (i.e. $\kappa C_I(\kappa)$; κ real) for each of these profiles. Here

$$C = C(\kappa) = C_R(\kappa) + iC_I(\kappa) \tag{19}$$

where C_R and C_I denote the real and imaginary parts of C, respectively. It is well known that in the temporally unstable range of κ, $C_R = U_c$.

Both growth-rate curves in figure 2 are quite close to each other and also to a parabolic shape with a neutral wavenumber of $2\kappa_0$ ($\cong 1$) and maximum growth rate of γ ($\cong 0.1$) occurring at the wavenumber κ_0 ($\cong 0.5$). We now replace the actual growth-rate curves by a single parabolic approximation (roughly the average of the two curves) and analytically continue the latter into the complex plane. Thus, for complex κ,

$$C(\kappa) = U_c - \frac{i\gamma}{\kappa_0^2}(\kappa - 2\kappa_0) \tag{20}$$

where U_c, γ, and κ_0 are suitable parameters associated with the instabilities of the base flow. The evolution equation for the phase becomes, via (7a) and (16b),

$$\frac{\partial\phi}{\partial\tau} + \frac{\partial\phi}{\partial\xi} C[\delta(\tau)(\phi_\xi^2 + \phi_\zeta^2)^{1/2}] = 0 \tag{21}$$

where $\phi_\xi = \partial\phi/\partial\xi$, $\phi_\zeta = \partial\phi/\partial\zeta$, and C, as a function of its argument, is given by (20). We shall solve (21) for the phase, $\phi = \phi(\xi, \tau)$.

After substituting (20) into (21), we obtain a first-order nonlinear partial differential equation for ϕ. The solution of this equation, obtained by standard methods (Courant & Hilbert 1966, p. 97) is conveniently written in the form

$$\phi = \phi(\xi, \tau) = -\frac{i\gamma}{\kappa_0^2}\,\phi_\xi(\phi_\xi^2 + \phi_\zeta^2)^{1/2}\, J(\tau) \tag{22a}$$

where

$$J = J(\tau) = \int_0^\tau \delta(\tau')\mathrm{d}\tau' \tag{22b}$$

is the integrated thickness of the mixing layer up to the current time.

In order to make the phase in (22a) an explicit function of ξ and τ, we must express the local wave vector, $\nabla\phi = (\phi_\xi, \phi_\zeta)$, as a function of these variables. This is done in Appendix A. A discussion of the results for the phase, wave vector, etc., will be provided in §6. The role of U_c, γ, and κ_0 in determining the dynamic similarity of the flow is explained in Appendix B. Note that the phase vanishes at the initial instant of time, $\tau = 0$, when the base flow is disturbed impulsively.

Some remarks are in order: First, it is possible to obtain $C = C(\kappa)$ numerically, tabulate these results on a grid in the complex κ-plane, and then use these tabulated values (with some form of interpolation) to solve (21) numerically. This we wanted to avoid, at least in the present study, in order to develop some analytical feel for the behavior of the phase and its secondary instabilities. Second, the approximation of the growth-rate curve by a parabola is quite good (even when γ is finite) and becomes the correct asymptotic limit for many flows in the vicinity of the critical value of an externally adjustable parameter that separates regions of stability from those of instability. Third, for a mixing layer, the maximum temporal growth rate itself is proportional to the velocity difference $\Delta U = U_1 - U_2$; $\gamma \cong 0.2\kappa_0\Delta U$ is a reasonable approximation for both the tanh and erf profiles (see (18) and (17a)). Finally, J/τ is the average thickness, say, $\bar{\delta} = \bar{\delta}(\tau)$, and the quantity $(\tau\delta/J)$, which appears throughout the analysis, may be interpreted as the ratio of the current (or 'local') and the average thickness, $\delta/\bar{\delta} \geq 1$.

5. The amplitude equation

With the solution for the complex phase out of the way, we now focus our attention on the equation for the wave action, (10a). One objective is to derive an interesting expression for H, under the assumption that we have a temporally spreading and self-similar base flow, as described in §3.

We begin with the group velocity, $\mathbf{G}$. After expressing the dispersion relation, $\Omega = \Omega(\mathbf{k}, \tau)$, in terms of the canonical phase speed $C = C(\kappa)$ via (16b), employing (20), (11), and our results for $\nabla\phi$ (see A 3,4), we obtain

$$\mathbf{G} = \left\{ \frac{\delta}{\bar{\delta}} \, \frac{\xi}{\tau} + U_c \left[1 - \frac{\delta}{\bar{\delta}} \right] + \frac{2i\gamma}{\kappa_0} \left[1 - \frac{\delta}{\bar{\delta}} \right] \right\} \mathbf{e}_1 + \frac{\delta}{\bar{\delta}} \, \frac{\zeta}{\tau} \, \mathbf{e}_3 \tag{23a}$$

and, from (23a),

$$\nabla \cdot \mathbf{G} = 2\, \delta/J \tag{23b}$$

It is rather easy to establish (23a) for two-dimensional disturbances (in which case only the first term on the right-hand side survives); however, for three-dimensional disturbances, considerable algebra is needed.

Note first that the group velocity is generally complex; the imaginary part of the streamwise component is proportional to the growth rate, γ, while the imaginary part of the spanwise component vanishes. Second, for a non-spreading base flow (i.e. $\delta/\bar{\delta} = 1$), the group velocity is actually real,

$$\mathbf{G} = \boldsymbol{\xi}/\tau \tag{24}$$

This result (i.e. (24)) is well known from the stationary-phase analysis of classical parallel flows (Gaster 1975). Interestingly enough then, wave packets in a spreading base flow differ in an *essential* way from those in non-spreading flows because of their complex group velocities; the physical implications of this will be discussed in §6 in terms of the secondary instabilities of the packet. Third, the divergence of the group velocity (i.e. $\nabla \cdot \mathbf{G} = 2\delta/J =$ real) is interpreted as the term responsible for the algebraic time-decay of the complex wave action; specifically, momentarily setting $H = 0$ in (10a) we find

$$\mathcal{A}J^2 = \text{const.} = \text{adiabatic invariant} \tag{25}$$

for an observer (formally) moving with the group velocity. In other words (or still with $H = 0$), $A \sim J^{-1}$, a result generalizing the classical stationary-phase analysis that gives $A \sim \tau^{-1}$ for a wave packet in a non-spreading base flow. For example, if $\delta \sim \tau^{1/2}$ due to the molecular diffusion of the base flow, $A \sim J^{-1} \sim \tau^{-3/2}$; therefore, the algebraic decay of the amplitude is enhanced owing to the effects of flow spreading. This effect is even stronger in a 'turbulent' flow where we might set $\delta \sim \tau$ so that $A \sim \tau^{-2}$. These simple scaling rules, especially when it is realized that $\xi \sim \tau$ for a convected wave packet in a spatially spreading base flow, make considerable sense physically.

Based on these opening remarks, we introduce

$$\mathcal{B} = \mathcal{A}J^2 \tag{26a}$$

where, in view of (10a), $\mathcal{B}$ satisfies

$$\frac{\partial \mathcal{B}}{\partial \tau} + \mathbf{G} \cdot \nabla \mathcal{B} + H\mathcal{B} = 0 \tag{26b}$$

and H is defined by (10c). We now obtain a more explicit representation for H; it is this coefficient that ultimately contains the most important interaction between the base flow and the inviscid wave packet. This interaction is completely absent in all classical theories of wave action.

First use (16) in the definitions of Q and $\mathbf{W}$, (9*b,c*) in order to write these equations in terms of the canonical pressure mode P; replace all y-derivatives and integrals with those involving η, use (7*a*), (8*a*), and (16*b*) and define

$$N(\kappa) = \int_{-\infty}^{\infty} \frac{U'''(\eta)}{[C(\kappa) - U(\eta)]^4} P(\eta, \kappa)P'(\eta, \kappa)\mathrm{d}\eta \tag{27a}$$

$$D(\kappa) = \int_{-\infty}^{\infty} \frac{1}{[C(\kappa) - U(\eta)]^3} \{[P'(\eta, \kappa)]^2 + \kappa^2 P^2(\eta, \kappa)\}\mathrm{d}\eta \tag{27b}$$

and

$$F(\kappa) = -\frac{N(\kappa)}{D(\kappa)} \tag{27c}$$

where the prime denotes differentiation with respect to η. Then from (10*c*), (5), and (12*a*) we find

$$H = \frac{F[\delta(\tau)(\phi_\xi^2 + \phi_\zeta^2)^{1/2}]}{\delta^2(\tau)} \tag{28}$$

After some integrations by parts in (27*a,b*) and invoking the Rayleigh equation, (14*a*), we arrive at a representation for $F(\kappa)$, namely,

$$F(\kappa) = \frac{\langle U'''' \rangle}{\langle U'' \rangle} \tag{29a}$$

where $\langle h \rangle$ denotes a mode-weighted average of $h = h(\eta)$, defined by

$$\langle h \rangle = \int_{-\infty}^{\infty} h(\eta) \frac{[P'(\eta, \kappa)]^2}{[C(\kappa) - U(\eta)]^4} \mathrm{d}\eta \tag{29b}$$

Of course, $\langle \cdot \rangle$ is a function of a single complex variable, say, κ.

Thus, apart from the scale factor δ^{-2}, the coefficient of $\mathcal{B}$ in (26*b*) is expressible as the ratio of the weighted averages of the fourth and second derivatives of the base velocity profile, $U = U(\eta)$, evaluated at $[\delta(\phi_\xi^2 + \phi_\zeta^2)^{1/2}]$. After substituting (A 3,4) for $\nabla\phi$ into (28), we get

$$H = H(\xi, \tau) \tag{30}$$

In §6 we discuss the behavior of F, both as $F = F(\kappa)$ and as $F = F(\xi, \tau)$, via the substitution $\kappa = \delta(\tau)(\phi_\xi^2 + \phi_\zeta^2)^{1/2}$.

A feature of (29a) is that $F(\kappa)$ is independent of the velocity ratio $(U_1 - U_2)/(U_1 + U_2)$. Therefore, H may be determined, once and for all, for each intrinsic velocity profile $f = f(\eta)$ (see (17), (18), and Appendix B). It is also important to appreciate the somewhat misleading form of (28), which arises because our base flow is self-similar; a more penetrating interpretation for δ^{-2} is $2\delta'/\delta$. This is valid whenever the base flow is spreading due to molecular diffusion (i.e. $\delta = (1 + \tau)^{1/2}$); here $\delta' = d\delta/d\tau$. Thus, H vanishes when δ' is zero (i.e. δ = const.), and for a self-similar profile this takes place as $\delta \to \infty$. These remarks make a great deal of sense physically.

Finally, observe that when κ equals the neutral wavenumber (say, $\kappa_n \cong 2\kappa_0$) both the numerator and denominator of (29a) possess a first-order pole at $\eta = 0$, and the integral in (29b) is to be evaluated by letting the contour of the integration pass below this pole in the complex η-plane. In fact, in this special case, the entire contribution to the integrals comes from the pole (i.e. the critical layer) because, for real η, the integrands in (29a) are odd functions of η. For this reason we can evaluate $F(\kappa_n)$ analytically. Thus we get a simple result that provides a check on the numerical results presented in §6.

6. Discussion of results

6.1. *The phase and wave vector*

From (22a) and (A 1,2) it is seen that both the complex phase, ϕ, and the local wave vector, $\nabla\phi$, may be written as products of temporal and spatial factors. Introduce

$$X = \frac{\xi}{\tau} - U_c \tag{31a}$$

$$Z = \frac{\zeta}{\tau} \tag{31b}$$

$$T = \tau \tag{31c}$$

and note that

$$\phi = \frac{\gamma T}{\bar{\delta}} \Phi(X, Z) \tag{32}$$

where $\bar{\delta} = \bar{\delta}(T) = J(T)/T$ is the average thickness and Φ, as a function of its arguments, can be calculated once and for all. We say that a 'fixed' point in the wave packet corresponds to $\mathbf{X} = (X, Z) =$ const., for example, the point $X = Z = 0$ is at the center of the packet.

Observe from (32) that for a non-spreading base flow with $\bar{\delta} = \delta =$ const. $= 1$, the phase is proportional to T so that the age of a disturbance is directly measured by its phase. On the other hand, for a spreading base flow, the phase varies less strongly with time because the average thickness of the layer, $\bar{\delta}$, is monotonically increasing with time. For large values of time, we estimate the phase to be proportional to $T^{1/2}$ and T^0 $=$ const., respectively, for 'laminar' (i.e. $\delta \sim T^{1/2}$) and 'turbulent' (i.e. $\delta \sim T$) diffusions of the base flow.

In accordance with the high-frequency ansatz, (6), the imaginary part of the phase, $\phi_I = \mathrm{Im}(\phi)$, is a measure of the magnitude of our exponentially growing disturbance on a log-scale. In view of our remarks in the preceding paragraph, the disturbance grows linearly initially, followed by a milder growth (such as a square root behavior) for larger values of time (all on a log-scale, of course). Clearly, the effect of base-flow spreading is to inhibit the growth of the disturbance, as expected intuitively, but in a base flow dominated by molecular diffusion, the disturbance continues to grow in magnitude for all values of time. This is very different from what happens to a single instability mode in a spreading base flow; such a mode always becomes 'neutral' for some finite value of time (or streamwise location), as demonstrated by Crighton & Gaster (1976). We shall provide a convincing explanation for this difference shortly.

In figure 3, we show contour plots of the real and imaginary parts of Φ as functions of (X, Z). It is important to recall that these plots are independent of time and represent the spatial factor of the phase (see (32)). With reference to figure 3(*b*), we see that $\mathrm{Im}(\Phi) = \Phi_I$ is negative in the central portion of this figure; thus the wave packet is unstable in this region. Furthermore, we may think of the closed curve $\Phi_I = 0$ as the boundary of the packet and the exponentially large disturbance near the middle of the packet diminishes with distance away from its center (at $\mathbf{X} = 0$). Within the footprint of the wave packet, the lines of constant phase, Φ_R = const., are practically parallel (see figure 3*a*), thereby indicating a wave structure whose wave fronts are perpendicular to the streamwise direction (and, in conjunction with figure 3*b*, a structure whose magnitude diminishes in the X and Z directions). These remarks are perfectly consistent with Balsa (1989a), in which a surface plot of a wave packet is provided in a constant-thickness mixing layer.

In figure 4 we show the spatial factors associated with the local wave vector $\nabla\phi$; these are obtained by pulling out the time factor, $\kappa_0/\bar{\delta}$, from $\nabla\phi$. In other words, we write

$$\nabla\phi = (\phi_\xi, \phi_\zeta) = \frac{\kappa_0}{\bar{\delta}}\,\mathbf{K}(X, Z) \tag{33a}$$

where $\mathbf{K} = (K, L)$ is the desired spatial factor.

We note from figure 4 that a large region near the center of the packet is dominated by a wave vector $\mathbf{K}$, whose real part is roughly (1, 0). Therefore, in this same region,

$$\mathrm{Re}(\nabla\phi) \cong \frac{\kappa_0}{\bar{\delta}}\,\mathbf{e}_1 \tag{33b}$$

so that the dominant wavenumber in the packet is continuously shifting to lower values with increasing time. This is clear physically: As the thickness of the mixing layer increases, the wave packet tries to adjust its length scale such that it stays in step with the local length scale of the base flow. Note that initially (at $T = 0$ with $\bar{\delta} = 1$) the dominant wavenumber in the packet is the most unstable wavenumber, κ_0, of temporal instability. Of course, as the thickness of the mixing layer increases, the local dispersion relation is shifting as well; it is possible to visualize this shift on figure 2(*b*). Roughly, with increasing time, both the maximum growth rate and the range of unstable wavenumbers diminish—the growth-rate parabola is effectively 'collapsing' toward the origin. A most important point to note is that this phenomenon is happening on the *local* or instantaneous thickness, $\delta = \delta(T)$, rather than on the average thickness, $\bar{\delta} = \bar{\delta}(T)$. Thus, at any instant of time, the maximum growth rate and the neutral wavenumber are given by

$$\gamma_{max} = \frac{\gamma}{\delta}, \quad \kappa_n = \frac{2\kappa_0}{\delta} \tag{34a,b}$$

We are now in a position to explain why the wave packet does not become neutral (or does not saturate) as a result of a spreading base flow caused by molecular diffusion. From (33*b*) and (34*b*), the ratio of the dominant instantaneous wavenumber at the center of the packet to the local neutral wavenumber is

$$\frac{\kappa_0/\bar{\delta}}{2\kappa_0/\delta} = \frac{\delta}{2\bar{\delta}} \to \frac{3}{4} \text{ as } \tau \to \infty \tag{35}$$

Thus, over the largest possible time interval, the dominant wavenumber of the packet shifts from the most unstable value to (roughly) half-way toward the neutral wavenumber. Therefore, a wave packet does not become neutral in a spreading base flow; in practical terms, a wave packet is likely to grow more violently than a pure instability mode in a given base flow. This is exactly what had been observed by Gaster (1981), although his qualitative explanation for this observation is very different from ours.

Since the total wavenumber, $(\phi_\xi^2 + \phi_\zeta^2)^{1/2}$, also plays an important role in our analysis, its corresponding spatial factor (i.e. $(\mathbf{K} \cdot \mathbf{K})^{1/2}$) is presented in figure 5. Very roughly, the real and imaginary parts are proportional to $(1 - Z^2\kappa_0^2/2\gamma^2)$ and $X\kappa_0/2\gamma$, respectively. It is possible to provide a much more accurate, though still approximate, representation of these quantities; this we shall not do for the sake of brevity.

6.2. *Complex wave action*

The equation that governs the evolution of the modal wave action is (26*b*); in the classical theories, $\mathscr{B}$ (of course, real in this case) would be the adiabatic invariant of the system. In the present analysis, $\mathscr{B}$ is no longer a conserved quantity because of the presence of a nonzero H. Thus

$$\frac{d\mathscr{B}}{d\tau} = \left[\frac{\partial}{\partial\tau} + \mathbf{G}\cdot\nabla\right]\mathscr{B} = -H\mathscr{B} \qquad (36a)$$

where $d/d\tau$ formally expresses time-differentiation for an observer moving with the group velocity. Our objective here is to shed some light on the evolution of $\mathscr{B}$ by examining the behavior of H, both in wavenumber space and in propagation space. Additionally, in the next sub-section, we discuss the implications of a complex group velocity vis-a-vis the secondary instability of the packet.

Since, from (28),

$$H = \frac{F[\delta(\tau)(\phi_\xi^2 + \phi_\zeta^2)^{1/2}]}{\delta^2(\tau)} \qquad (36b)$$

we start with a discussion of $F = F(\kappa)$. This complex quantity, as a function of (complex) κ, has been evaluated numerically from its definition, (29*a*), for both the tanh and the erf profiles. The results are presented in figures 6 and 7.

Note first from figure 5 that the real part of the spatial factor associated with the total wavenumber, $(\phi_\xi^2 + \phi_\zeta^2)^{1/2}$, varies from 0 to 1 while its imaginary part varies from -1 to 1. Essentially, the complex argument of F in (36*b*) ranges over the Cartesian product $(0, 3\kappa_0/2) \times (-3\kappa_0/2, 3\kappa_0/2)$. In this domain, $\mathrm{Re}(F) = \delta^2\mathrm{Re}(H)$ is negative so that the effect of base-flow spreading is to *increase* the magnitude of $\mathscr{B}$; this increase is algebraic on the slow viscous time scale, τ, and its order of magnitude is very roughly

τ^4 near the center of the packet. Thus, owing to flow divergence, the disturbance is capable of extracting additional energy from the base flow via Reynolds stresses evolving on the long spatial and temporal scales. Because of the strong similarity of figures 6(*a*) and 6(*b*) for the tanh and erf profiles, we believe that our previous conclusion is quite general. As mentioned already, at the neutral point, $\kappa = \kappa_n$, F may be evaluated analytically; these values are -8 and -6 for the tanh and erf profiles, respectively. These theoretical results are entirely consistent with those given in figure 6.

In figure 7, we show the behavior of $\mathrm{Re}\{F[\delta(\phi_\xi^2 + \phi_\zeta^2)^{1/2}]\}$ in propagation space, **X**, for three values of time (τ = 0, 2, and 10). These results are obtained by combining those in figures 5 and 6. Because of the temporal factor associated with the argument of F in the expression above, Re(F) is time dependent; however, this time dependence is relatively slow in comparison with the variation of δ^{-2} in (36*b*). Thus, near the center of the packet, $\mathscr{B}^{-1}\, d\mathscr{B}/d\tau \cong$ const./$(1 + \tau)$, where the real value of this constant of proportionality is about 4 at early times and is around 5 at large times. This results in an algebraic growth of the wave action $\mathscr{B}$, as discussed previously.

In order to understand more fully the evolution of the wave action and the role of a complex group velocity, we perform a number of manipulations on the governing equation, (26*b*). First invoke coordinate transformation (31) and introduce a new time, $\mathscr{T}$,

$$\mathscr{T} = \log \bar{\delta}(T) \qquad \text{when } d\delta/d\tau > 0 \tag{37a}$$

so that (26*b*) may be thrown into the form

$$\frac{\partial \mathscr{B}}{\partial \mathscr{T}} + \left[X - \frac{2i\gamma}{\kappa_0}\right] \frac{\partial \mathscr{B}}{\partial X} + Z\,\frac{\partial \mathscr{B}}{\partial Z} + \frac{J(T)}{\delta(T) - \bar{\delta}(T)}\, H\, \mathscr{B} = 0 \tag{37b}$$

This transformation fails when the base flow is not spreading since (37*a*) is meaningless. Second, separate (37*b*) into its real and imaginary parts and then extend this 2×2 system of real equations into the complex plane by writing

$$X \to X + iY \tag{38a}$$

$$\mathcal{B}_{\mathrm{R}}(X, Z, \mathcal{T}) \to \mathcal{B}_{\mathrm{R}}(X + iY, Z, \mathcal{T}) = B_1(X, Y, Z, \mathcal{T}) \tag{38b}$$

and

$$\mathcal{B}_{\mathrm{I}}(X, Z, \mathcal{T}) \to \mathcal{B}_{\mathrm{I}}(X + iY, Z, \mathcal{T}) = B_2(X, Y, Z, \mathcal{T}) \tag{38c}$$

with similar expressions for $H = H_{\mathrm{R}} + iH_{\mathrm{I}} = (H_{\mathrm{R}}, H_{\mathrm{I}}) \to (H_1, H_2)$. Our basic unknown now is the complex two-vector $\mathbf{B} = (B_1, B_2)$; it satisfies the Cauchy-Riemann equations. Because of this, we can selectively eliminate $\partial/\partial X$ in favor of $\partial/i\partial Y$ and rearrange (37b) as

$$\frac{\partial \mathbf{B}}{\partial \mathcal{T}} + X \frac{\partial \mathbf{B}}{\partial X} + \begin{bmatrix} Y, & \dfrac{2\gamma}{i\kappa_0} \\ -\dfrac{2\gamma}{i\kappa_0}, & Y \end{bmatrix} \frac{\partial \mathbf{B}}{\partial Y} + Z \frac{\partial \mathbf{B}}{\partial Z} + \frac{J(T)}{\delta(T) - \bar{\delta}(T)} \begin{bmatrix} H_1, & -H_2 \\ H_2, & H_1 \end{bmatrix} \mathbf{B} = 0 \tag{39}$$

Finally, it is important to realize that Y has nothing to do with the cross-space coordinate y, and any physically meaningful solution of (39) must be evaluated at $Y = 0$.

The most important difference between (37b) and (39) is that the former equation is elliptic (with complex characteristics) whereas the latter is a symmetric hyperbolic system (actually hermitian) with real characteristics. In fact, if the characteristics of (39) are the level surfaces $\Psi(X, Y, Z, \mathcal{T}) = \text{const.}$, then Ψ satisfies

$$\left[\frac{\partial}{\partial \mathcal{T}} + X \frac{\partial}{\partial X} + Y \frac{\partial}{\partial Y} + Z \frac{\partial}{\partial Z}\right]\Psi \mp \frac{2\gamma}{\kappa_0} \frac{\partial \Psi}{\partial Y} = 0 \tag{40}$$

and thus the parametric representation of the ($\pm$) bicharacteristics of (39) are

$$\mathcal{T} = \sigma \tag{41a}$$

$$X = X_0 e^{\sigma} \tag{41b}$$

$$Y = Y_0 e^{\sigma} \pm \frac{2\gamma}{\kappa_0}(1 - e^{\sigma}) \tag{41c}$$

$$Z = Z_0 e^{\sigma} \tag{41d}$$

where σ (= $\mathscr{T}$) is the parameter and (X_0, Y_0, Z_0) represents a point on the bicharacteristic curve at the initial instant of time, $\tau = T = \mathscr{T} = 0$. In essence, these bicharacteristics may be interpreted as the real rays arising from the complex group velocity associated with (26*b*) (or, actually, more precisely with (37*b*)).

In order to obtain the solution at an arbitrary point, P = (X, Y = 0, Z), for a certain value of time (say, $\mathscr{T} = \sigma$), we construct the two 'backward-running' bicharacteristics in order to pick up the initial point, (X_0, Y_0, Z_0), via (41) (see figure 8 for the geometry). At this point the initial value of **B** is available from the analytic continuation of the specified initial data in propagation space. Note that even though $Y = 0$, $Y_0 \neq 0$, so that in order to obtain the physical solution at P we *must* have the analytic continuation of the initial data at hand. We shall implicitly assume that this continuation is always possible.

Along each of the (±) bicharacteristics, (39) reduces to a first-order, linear, ordinary differential equation for the corresponding characteristic variable, ($B_1 \pm iB_2$). Each of these equations may be solved by elementary methods involving the quadratures of H_1 and H_2. The general qualitative nature of this solution has been anticipated earlier in this sub-section.

It is important to realize that, because of the complex group velocity, there are actually *two* rays (or *bicharacteristics*) passing through each point in propagation space. The projection of these rays onto propagation space is a radial line; the two rays are indistinguishable in this space.

6.3. *Secondary instabilities*

Because the group velocity is complex, (37*b*) is a real 2×2 elliptic system for $\mathscr{B}$ = ($\mathscr{B}_R$, $\mathscr{B}_I$). For such a system, the initial value problem at $\tau = T = \mathscr{T} = 0$ is 'ill posed' in the sense of Hadamard, although for analytic initial data, a properly posed solution exists, at least locally in the immediate neighborhood of the initial hypersurface. We interpret the global ill-posedness as the secondary instability of the wave packet.

In the preceding sub-section we have transformed this ill-posed elliptic system into a well-posed hyperbolic system. This transformation is somewhat misleading because the analytic continuation of the initial data is, in itself, an unstable process (more about this later); specifically a typical rapid, but perhaps spurious, oscillation of wavenumber $n\kappa_0$ ($n >> 1$) along the X-axis is converted into an exponentially large value when analytically continued into the complex plane, beyond the strip $|Y| = O(1/n\kappa_0)$. The two crucial heuristic questions are these: (a) How far do we need to continue the initial data into the complex plane in order to describe the evolution of the complex wave action for all values of time? (b) What is the role of the group velocity in advecting spurious disturbances away from the footprint of the packet, which, after all, is confined to a fairly small region in (X, Z) space (see figure 3)? We will be able to answer both of these questions quite satisfactorily by considering the secondary instabilities of the packet.

In order to accomplish this, we perturb the phase by a small quantity, ψ, so that

$$\text{Total Phase} \rightarrow \phi + \psi \tag{42a}$$

where ϕ is given by (22a). Since the total phase satisfies dispersion relation (7a), it is a simple matter to show by linearization that the perturbation phase, ψ, satisfies

$$\frac{\partial \psi}{\partial \tau} + \mathbf{G} \cdot \nabla \psi = 0 \tag{42b}$$

This equation is exactly the same as (36a) with $H = 0$, so that the previous discussion on analytic continuation is applicable to (42b). For example, if $\psi_j^{(0)}(X, Y, Z)$ ($j = 1, 2$) represent, respectively, the analytic continuation of the initial data, $\psi_\nu^{(0)}(X, Z)$ (ν = R = real; ν = I = imaginary parts), then by the method of characteristics outlined in §6.2, the solution for the analytic continuation of $\psi_R \rightarrow \psi_1$ is

$$\psi_1(X, Y, Z, \mathcal{T}) = \frac{1}{2}\left\{\psi_1^{(0)}\left[Xe^{-\mathcal{T}}, Ye^{-\mathcal{T}} - \frac{2\gamma}{\kappa_0}(e^{-\mathcal{T}} - 1), Ze^{-\mathcal{T}}\right]\right.$$

$$\left. + \psi_1^{(0)}\left[Xe^{-\mathcal{T}}, Ye^{-\mathcal{T}} + \frac{2\gamma}{\kappa_0}(e^{-\mathcal{T}} - 1), Ze^{-\mathcal{T}}\right]\right\}$$

$$+ \frac{i}{2}\left\{\psi_2^{(0)}\left[Xe^{-\mathcal{T}}, Ye^{-\mathcal{T}} - \frac{2\gamma}{\kappa_0}(e^{-\mathcal{T}} - 1), Ze^{-\mathcal{T}}\right]\right.$$

$$\left. - \psi_2^{(0)}\left[Xe^{-\mathcal{T}}, Ye^{-\mathcal{T}} + \frac{2\gamma}{\kappa_0}(e^{-\mathcal{T}} - 1), Ze^{-\mathcal{T}}\right]\right\} \qquad (43)$$

A similar equation holds for ψ_2 (i.e. $\psi_1 \to \psi_2$); these equations are valid for all values of time.

The formal similarity between (43) and the classical D'Alembert solution for the simple wave equation is absolutely striking. Apparently the initial data split into two halves; each of these propagates along one of the bicharacteristics, and these two halves add (or subtract) at subsequent instants of time to form the required solution.

We are now ready to answer the two questions raised previously. For large values of time, $\mathcal{T} \to \infty$, the physically valid solution at a fixed (X, Z) is

$$\psi_1(X, 0, Z, \mathcal{T}) = \frac{1}{2}\left\{\psi_1^{(0)}\left[0, \frac{2\gamma}{\kappa_0}, 0\right] + \psi_1^{(0)}\left[0, -\frac{2\gamma}{\kappa_0}, 0\right]\right\}$$

$$+ \frac{i}{2}\left\{\psi_2^{(0)}\left[0, \frac{2\gamma}{\kappa_0}, 0\right] - \psi_2^{(0)}\left[0, -\frac{2\gamma}{\kappa_0}, 0\right]\right\} \qquad (44a)$$

$$\psi_2(X, 0, Z, \mathcal{T}) = \frac{1}{2}\left\{\psi_2^{(0)}\left[0, \frac{2\gamma}{\kappa_0}, 0\right] + \psi_2^{(0)}\left[0, -\frac{2\gamma}{\kappa_0}, 0\right]\right\}$$

$$- \frac{i}{2}\left\{\psi_1^{(0)}\left[0, \frac{2\gamma}{\kappa_0}, 0\right] - \psi_1^{(0)}\left[0, -\frac{2\gamma}{\kappa_0}, 0\right]\right\} \qquad (44b)$$

Since $\mathcal{T}$ is a logarithmic time scale, (see (37*a*)), the asymptotic result represented in (44) is actually attained only algebraically fast on the physical time scales τ or T.

The physical interpretation of (44) is this: An arbitrary initial disturbance in the phase is advected away from the footprint of the wave packet by the real part of the group velocity. This advection is radially outward in propagation space so that any disturbance that is *not* at $\mathbf{X} = (X, Z) = 0$ will be convected out of the packet. Therefore, the solution for large values of time will be dominated by the initial disturbance near $\mathbf{X} = 0$; this disturbance cannot be advected away since the real part of the group velocity vanishes at the origin. More precisely, it is the analytic continuation of this initial data into the interval $|Y| \leq 2\gamma/\kappa_0$ that actually matters. Therefore, a spurious rapid oscillation of the phase at a characteristic wavenumber, $n\kappa_0$ ($n >> 1$), will attain the value $\exp(2n\gamma)$ for very large values of time.

This result is interesting. It says that perturbations of the phase will saturate; therefore, at large values of time, the total phase will be dominated by ϕ. This is exact in the linear theory. In other words, as $\mathcal{T} \to \infty$, $\psi \to \psi_\infty$ (= complex const.) so that the complex phase, ϕ, jumps by fixed amounts as a result of the asymptotic response to the perturbations in the phase.

On the other hand, it is easy to see from (43) that for small (or moderate) values of time, the above-mentioned rapid oscillations in the phase will grow as $\exp(2n\gamma\tau)$. This observation, combined with the fact that the actual problem is *nonlinear*, strongly suggests that once these small-scale, rapidly growing (though only initially) disturbances are triggered in the flow, they will lead to the secondary instabilities of the wave packet.

It is also possible to study the evolution of small disturbances riding on top of the wave action, $\mathcal{B}$, by writing

$$\text{Total Wave Action} \to \mathcal{B} + \beta \tag{45}$$

where β is the perturbation. After substituting (45) and (42*a*) into (26*b*) and linearizing, we arrive at an equation for β. This equation is very similar to (26*b*); essentially H is replaced by derivatives of F and $\mathbf{G} = \partial\Omega/\partial\mathbf{k}$ with respect to the wave vector, because of the perturbations in the phase. It is beyond the scope of this paper to study the solutions of this equation; we plan to examine this equation in a forthcoming paper in which we will study the secondary instabilities of an instability mode (rather than a wave packet).

7. Conclusions

It is well known that an instability mode evolving in a spreading base flow attains a neutral state at some streamwise location. This is not the case for a wave packet: The dominant wavenumber in a packet is such that the local growth rate associated with it is in the vicinity of the maximum growth rate of the local dispersion relation. Although there is some shift toward the neutral wavenumber (and away from the most unstable one), this shift is far from complete even as τ (or ξ) $\rightarrow \infty$. For this reason, a wave packet is expected to grow more violently than an instability mode in a given spreading base flow.

The wave action, $\mathcal{B}$, is no longer a conserved quantity; because of the interaction between the base flow and the disturbance, $\mathcal{B}$ grows algebraically on the slow time scale, τ. The group velocity is complex, and the equation for the wave action may be converted into a symmetric hyperbolic system via analytic continuation. We use this hyperbolic system to study the behavior of the perturbed phase. It is found that small-scale disturbances to the phase grow very rapidly initially and then saturate at later values of time. We interpret this initial growth as the secondary instability of the packet.

The author is grateful for the financial support provided by the Institute for Computational Mechanics in Propulsion (ICOMP). He also expresses his thanks for the hospitality provided by the NASA Lewis Research Center during a summer (1993) visit, and to M. E. Goldstein and L. S. Hultgren for numerous discussions on hydrodynamic stability.

Appendix A. Dependence of wave vector on space and time

We obtain a formal solution to (21) using the characteristic differential equations belonging to (21). Since the wave vector, $\nabla\phi$, is constant along the complex rays, the trajectory of these rays may be solved for quite simply, with the initial condition that all rays emanate from the spatially compact source of the disturbance at $\xi = 0$. We express the equations of the rays in (ξ, τ) space as

$$\frac{\xi - U_c\tau - 2i\gamma\tau/\kappa_0}{i\gamma J/\kappa_0^2} = -(\phi_\xi^2 + \phi_\zeta^2)^{1/2} - \frac{\phi_\xi^2}{(\phi_\xi^2 + \phi_\zeta^2)^{1/2}} \tag{A 1}$$

$$\frac{\zeta}{i\gamma J/\kappa_0^2} = -\frac{\phi_\xi\phi_\zeta}{(\phi_\xi^2 + \phi_\zeta^2)^{1/2}} \tag{A 2}$$

where the wave vector $\nabla\phi = (\phi_\xi, \phi_\zeta)$ may be thought of as the label that identifies a specific ray in propagation space (or, more precisely, in the analytic continuation of this space).

In order to obtain $\nabla\phi$ as a function of ξ and τ, we must invert (A 1,2). Let a and b temporarily denote the left-hand sides of (A 1,2), respectively. We first form the ratio (a/b), rearrange this to obtain a quadratic equation for (ϕ_ζ/ϕ_ξ) whose solution, in conjunction with (A 1,2), yields

$$\phi_\xi = \frac{[a^2 + 4b^2 + aS]^{1/2}}{2\sqrt{2}} \tag{A 3}$$

$$\phi_\zeta = \frac{[a^2 - 2b^2 - aS]^{1/2}}{\sqrt{2}} \tag{A 4}$$

and

$$\phi_\xi(\phi_\xi^2 + \phi_\zeta^2)^{1/2} = \frac{[a^4 + 20a^2b^2 - 8b^4 + aS^3]^{1/2}}{4\sqrt{2}} \tag{A 5}$$

where

$$S = (a^2 - 8b^2)^{1/2} \tag{A 6}$$

The outside square root on the right-hand side of (A 5) is chosen such that $\mathrm{Im}(\phi) = \phi_1 < 0$ (see (6) and (22*a*); thus we have an exponential instability), while the other fractional powers in (A 3,4) and (A 6) are chosen so that, in the first place, ϕ_ξ and ϕ_ζ are analytic functions of $\boldsymbol{\xi} = (\xi, \zeta)$ and that, second, the spatial derivatives of ϕ, as obtained from (22*a*), are equal to (A 3,4). Although it is cumbersome to verbally express these constraints on the fractional powers, it is simple to program them on a computer by examining the alternatives in 'if statements.'

In essence, (A 3,4) provide $\nabla\phi$ as functions of $(\boldsymbol{\xi}, \tau)$ and, when these functions are substituted into (22*a*), we obtain $\phi = \phi(\boldsymbol{\xi}, \tau)$. This is the desired result for the phase.

Appendix B. Dynamic similarity and scale transformation

The theory outlined in the main body of this paper contains three free parameters (see 20): the convection speed, $U_c = (U_1 + U_2)/2$; the maximum growth rate associated with the canonical dispersion relation, $\gamma \cong 0.2\kappa_0(U_1 - U_2)$; and the corresponding temporal wavenumber, $\kappa_0 \cong 0.5$. The numbers just provided for γ and κ_0 are reasonably accurate for both the tanh and erf profiles (see (17) and (18)).

What we wish to emphasize here is that the dependence on these three parameters can be eliminated completely by the introduction of new space variables. Very briefly, from (A 1,2), (31), and (A 3,4), we see that

$$\nabla\phi = \frac{\kappa_0}{\delta} \text{ (spatial factor)} \tag{B 1}$$

where the (spatial factor) in (B 1), essentially $\mathbf{K}$ of (33*a*), depends only on the variables $X\kappa_0/\gamma$ and $Z\kappa_0/\gamma$. Note that X and Z have physical units of speed, and a most important speed that totally governs dynamic similarity is the 'instability speed,' $\gamma/\kappa_0 \sim \Delta U = (U_1 - U_2)$.

Similar remarks hold for the spatial factor of the phase, (32), and the group velocity, (23*a*), relative to the convection speed

$$\frac{\mathbf{G} - U_c \mathbf{e}_1}{\gamma/\kappa_0} = \left\{ \frac{\delta}{\bar{\delta}} \frac{X\kappa_0}{\gamma} + 2i\left[1 - \frac{\delta}{\bar{\delta}}\right] \right\} \mathbf{e}_1 + \frac{\delta}{\bar{\delta}} \frac{Z\kappa_0}{\gamma} \mathbf{e}_3 \tag{B 2}$$

Once again we see from (B 2) the importance of the instability speed, γ/κ_0, in the normalization of the group velocity. Clearly, any physical mechanism of 'dispersion' for an instability wave packet is necessarily *very* different from that for a classical packet in a conservative system. Because of this scale transformation of $\mathbf{X} = (X, Z)$, all the results presented in figures 3-5 are essentially valid for arbitrary U_c, γ, and κ_0.

REFERENCES

ANDREWS, D. G. & MCINTYRE, M. E. 1978 On wave-action and its relatives. *J. Fluid Mech.* **89**, 647-664.

BALSA, T. F. 1988 On the receptivity of free shear layers to two-dimensional external excitation. *J. Fluid Mech.* **187**, 155-177.

BALSA, T. F. 1989a Three-dimensional wave packets and instability waves in free shear layers and their receptivity. *J. Fluid Mech.* **201**, 77-97.

BALSA, T. F. 1989b Amplitude equations for wave packets in slightly inhomogeneous unstable flows. *J. Fluid Mech.* **204**, 433-455.

BALSA, T. F. 1994 A note on the wave action density of a viscous instability mode on a diverging free shear flow. *J. Fluid Mech.* (submitted).

BETCHOV, R. & SZEWCZYK, A. 1963 Stability of a shear layer between parallel streams. *Phys. Fluids* **6**, 1391-1396.

COURANT, R. & HILBERT, D. 1966 *Methods of Mathematical Physics*. Interscience.

CRIGHTON, D. G. & GASTER, M. 1976 Stability of slowly diverging jet flow. *J. Fluid Mech.* **77**, 397-413.

CRIMINALE, W. O. & KOVASZNAY, L. 1962 The growth of localized disturbances in a laminar boundary layer. *J. Fluid Mech.* **12**, 59-80.

DRAZIN, P. G. & REID, W. H. 1981 *Hydrodynamic Stability.* Cambridge University Press.

GASTER, M. 1975 A theoretical model of a wave packet in the boundary layer on a flat plate. *Proc. R. Soc. Lond.* A **347**, 271-289.

GASTER, M. 1981 Propagation of linear wave packets in laminar boundary layers. *AIAA Journal* **19**, 419-423.

GASTER, M. & GRANT, I. 1975 An experimental investigation of the formation and development of a wave packet in a laminar boundary layer. *Proc. R. Soc. Lond.* A **347**, 253-269.

GASTER, M., KIT, E. & WYGNANSKI, I. 1985 Large-scale structures in a forced turbulent mixing layer. *J. Fluid Mech.* **150**, 23-29.

GOLDSTEIN, M. E. & LEIB, S. J. 1988 Nonlinear roll-up of externally excited free shear layers. *J. Fluid Mech.* **191**, 481-515.

HAYES, W. D. 1970 Conservation of action and modal wave action. *Proc. R. Soc. Lond.* A **320**, 187-208.

HULTGREN, L. S. 1992 Nonlinear spatial equilibration of an externally excited instability wave in a free shear layer. *J. Fluid Mech.* **236**, 635-664.

ITOH, N. 1981 Secondary instability of laminar flows. *Proc. R. Soc. Lond.* A **375**, 565-578.

LANDAHL, M. T. 1982 The application of kinematic wave theory to wave trains and packets with small dissipation. *Phys. Fluids* **25**, 1512-1516.

MASLOWE, S. A. 1981 Shear flow instabilities and transition. In *Hydrodynamic Instabilities and the Transition to Turbulence* (ed. H. L. Swinney & J. P. Gollub). Springer-Verlag.

TAM, C. K. 1967 A note on disturbances in slightly supercritical plane Poiseuille flow. *J. Fluid Mech.* **30**, 17-20.

WHITHAM, G. B. 1974 *Linear and Nonlinear Waves.* Wiley.

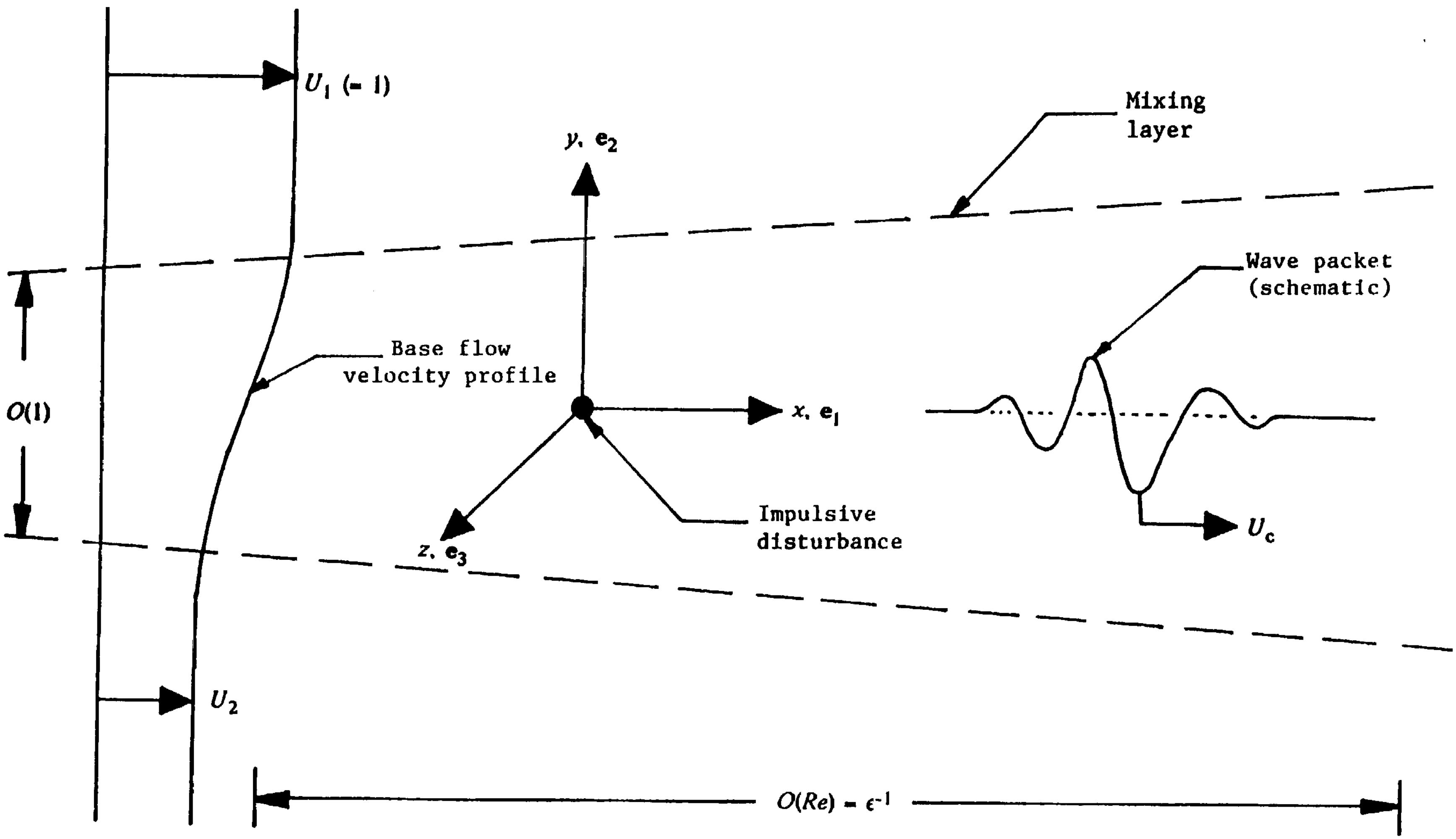

Figure 1. Geometry of problem (not to scale). y = cross space; (x, z) = propagation space.

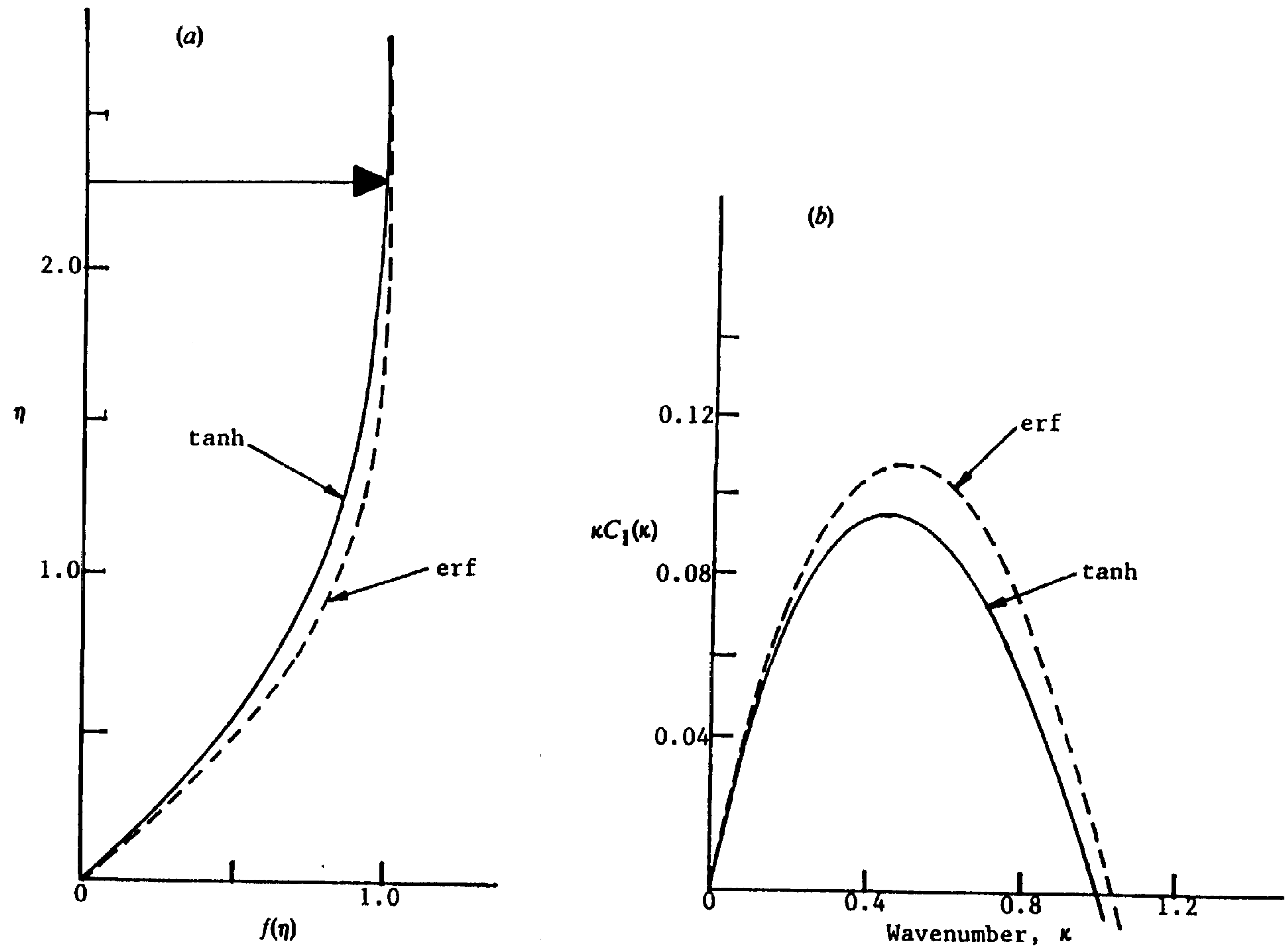

Figure 2. Representative base flow velocity profiles and growth rate curves: (*a*) tanh(η) and erf(η) profiles; (*b*) canonical growth rate as a function of wavenumber for erf and tanh profiles ($U_1 = 1$, $U_2 = 0$).

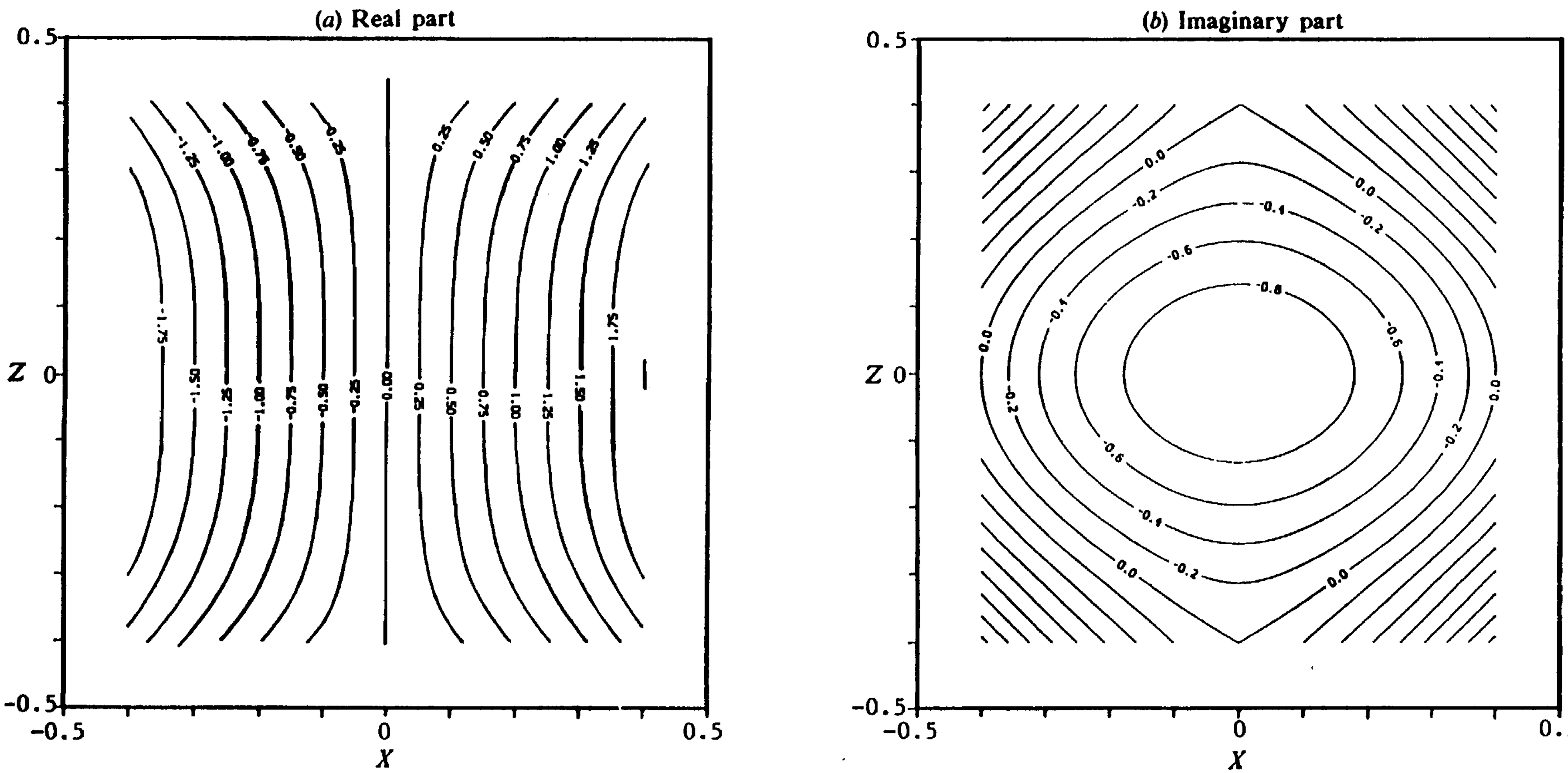

Figure 3. Contours of constant phase, Φ, in the wave packet ($U_1 = 1$, $U_2 = 0$, $\gamma = 0.1$, $\kappa_0 = 0.5$): (*a*) Φ_R = const.;

(*b*) Φ_I = const.

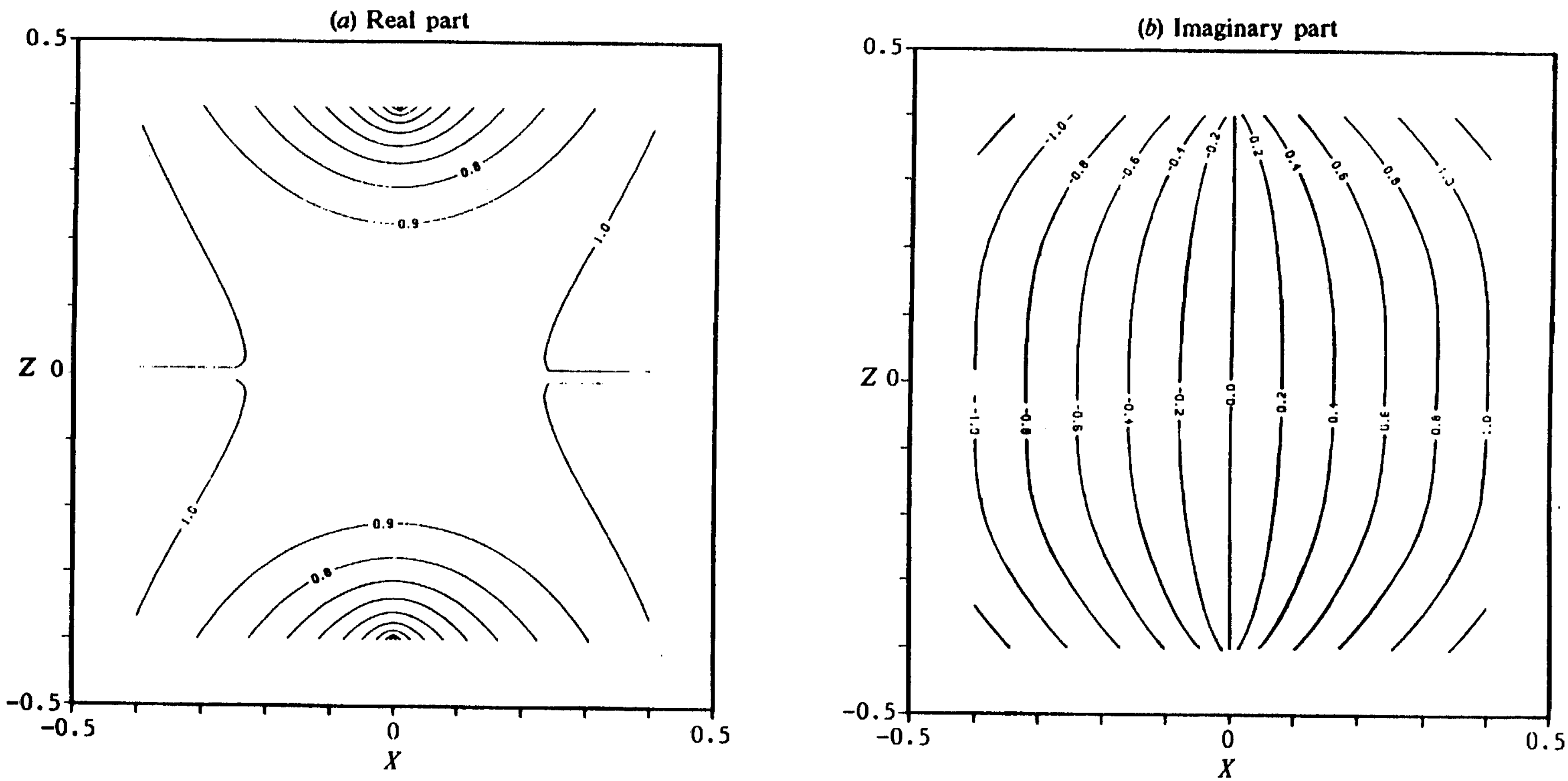

Figure 4. Contours of constant streamwise, K, and spanwise, L, wavenumbers in the wave packet ($U_1 = 1$, $U_2 = 0$, $\gamma = 0.1$, $\kappa_0 = 0.5$): (a) K_R = const.; (b) K_I = const.; (c) L_R = const.; (d) L_I = const.

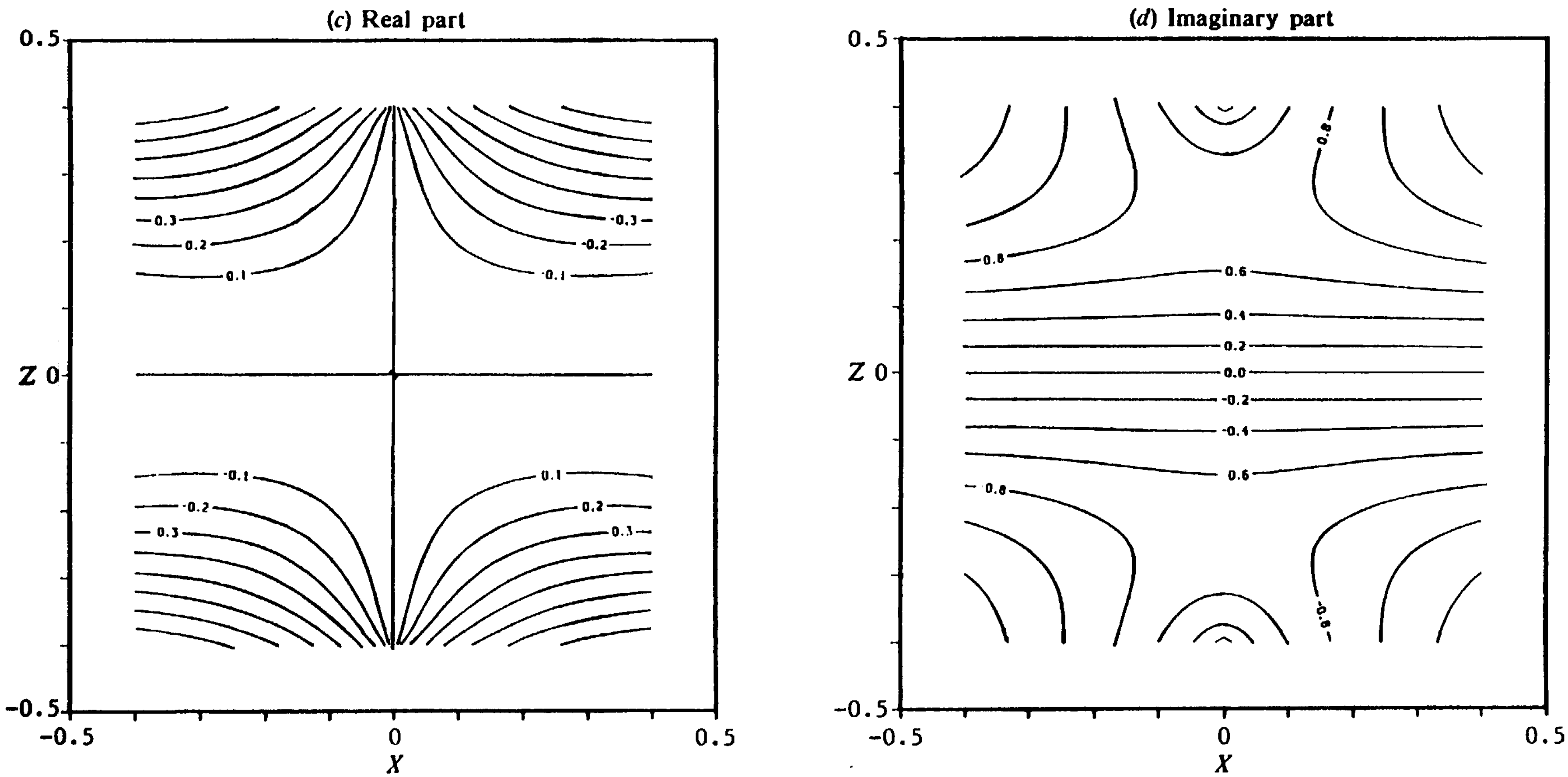

Figure 4. Continued.

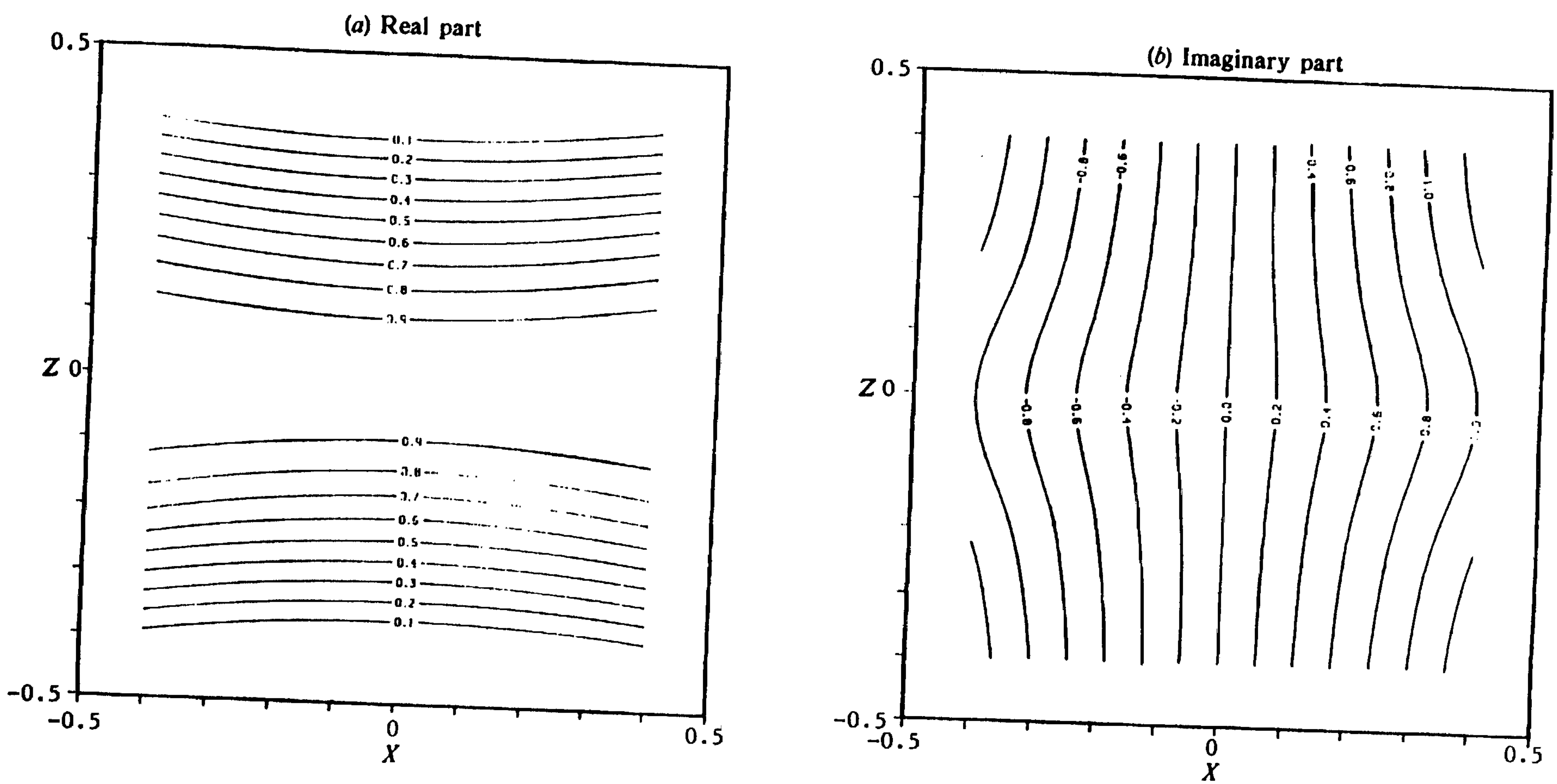

Figure 5. Contours of the spatial factor associated with the total wavenumber $(\phi_\xi^2 + \phi_\zeta^2)^{1/2}$ ($U_1 = 1$, $U_2 = 0$, $\gamma = 0.1$, $\kappa_0 = 0.5$): (a) real part; (b) imaginary part.

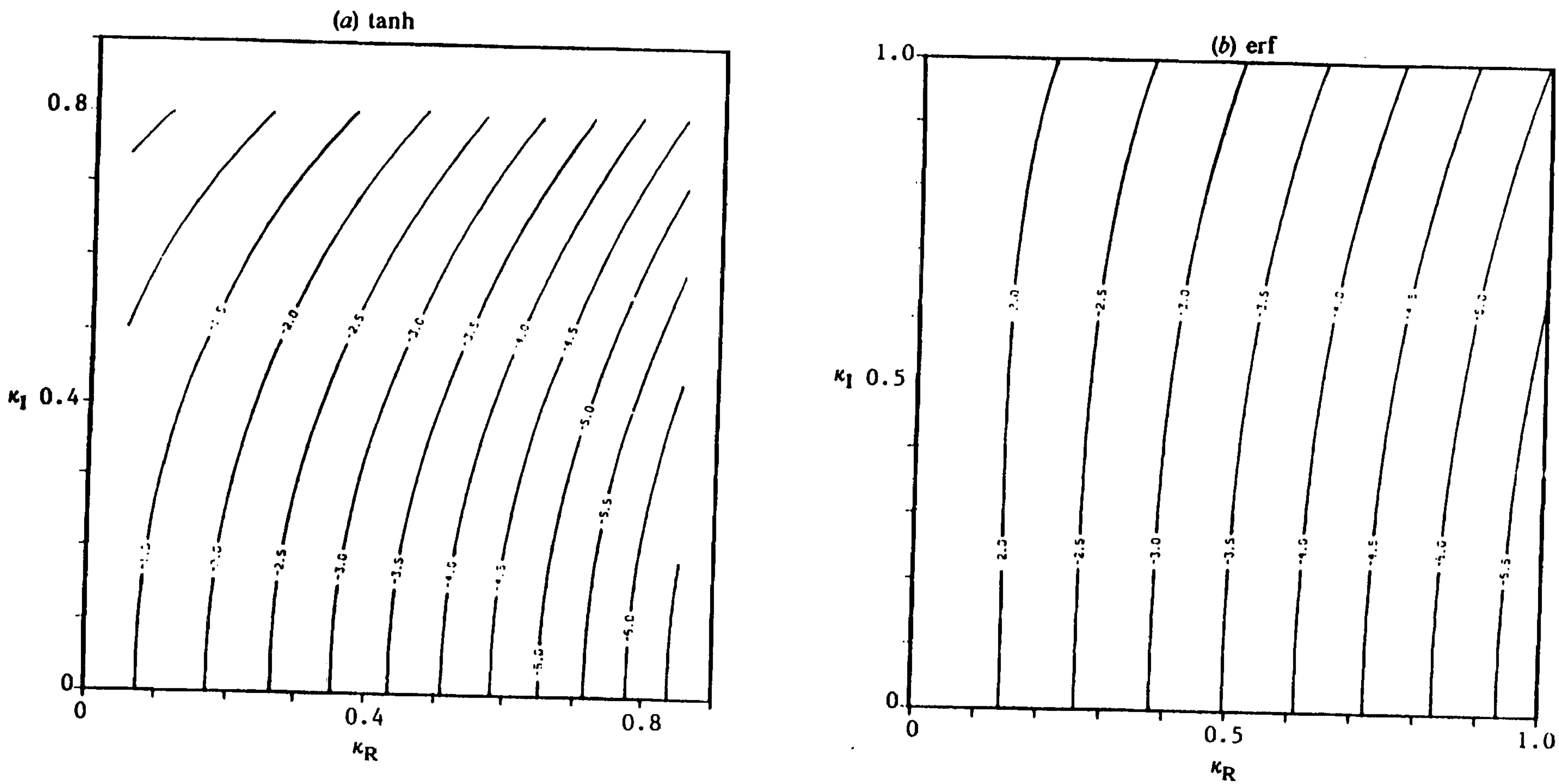

Figure 6. Contours of base-flow and wave-packet interaction function in wavenumber space--real parts: (*a*) tanh profile; (*b*) erf profile. (The contours are symmetric about the real axis for $\kappa_I < 0$).

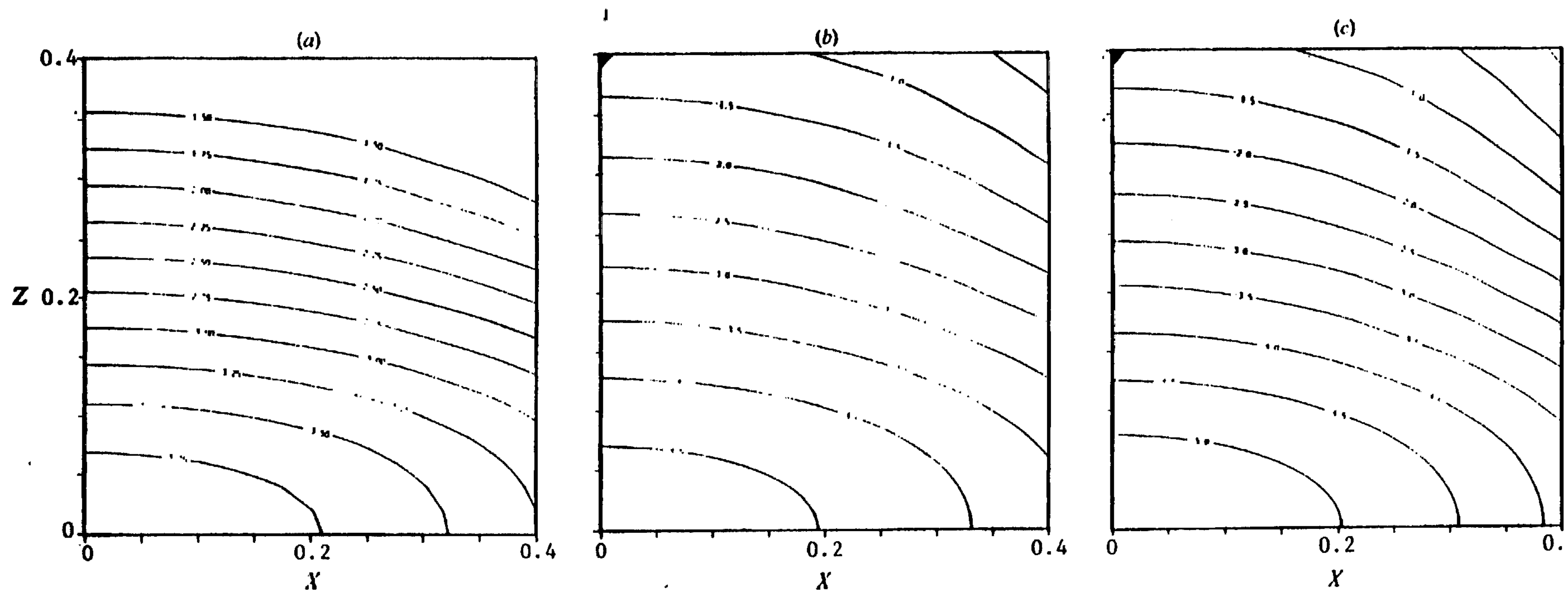

Figure 7. Contours of base-flow and wave-packet interaction function in propagation space--real parts for tanh profile ($U_1 = 1$, $U_2 = 0$; $\gamma = 0.1$; $\kappa_0 = 0.5$): (a) $\tau = 0$; (b) $\tau = 2$; (c) $\tau = 10$.

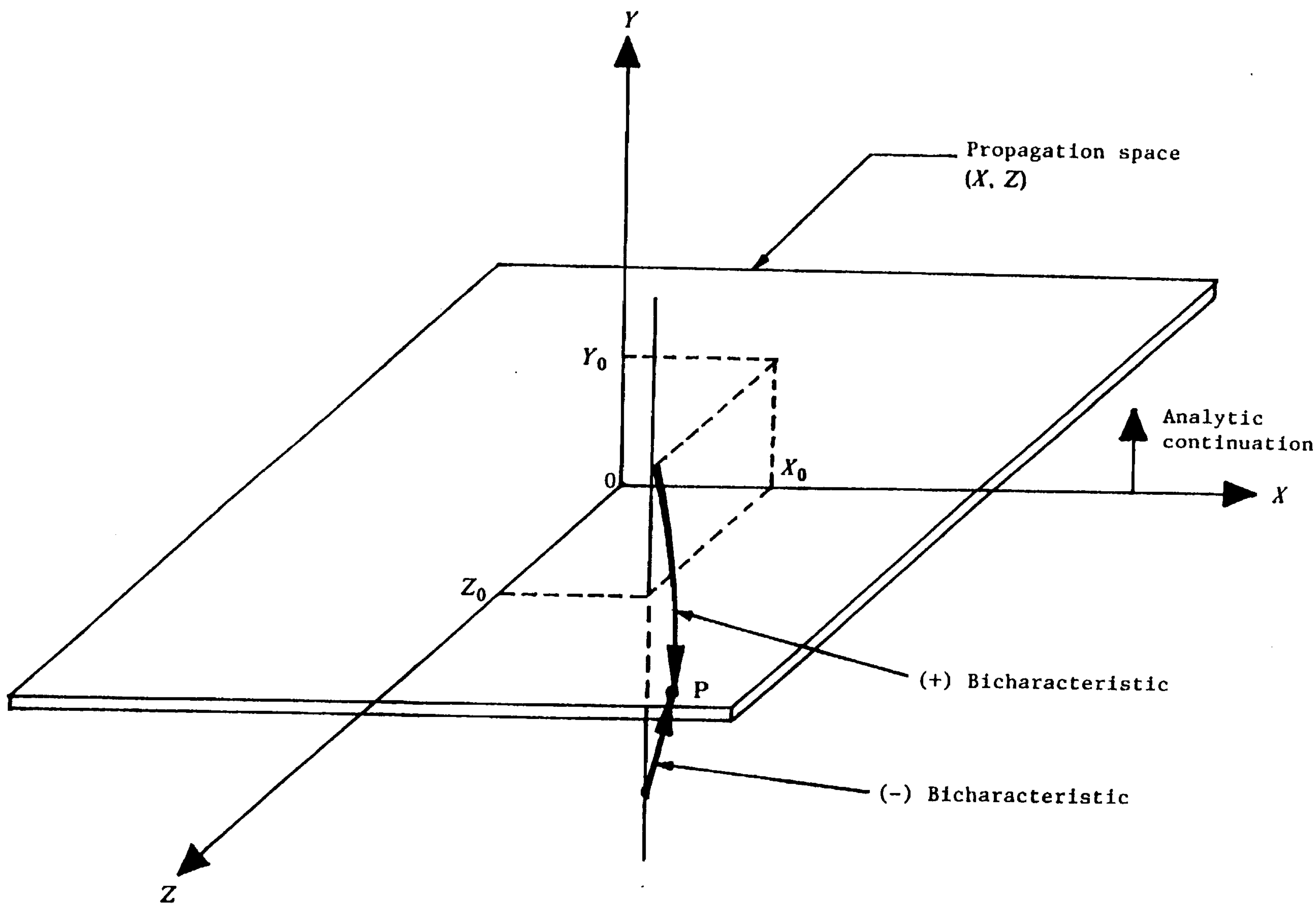

Figure 8. Bicharacteristics (rays) in the analytic continuation of propagation space.

REPORT DOCUMENTATION PAGE

Form Approved
OMB No. 0704-0188

1. AGENCY USE ONLY (*Leave blank*)	2. REPORT DATE	3. REPORT TYPE AND DATES COVERED
	November 1994	Technical Memorandum

4. TITLE AND SUBTITLE

On the Behavior of Three-Dimensional Wave Packets in Viscously Spreading Mixing Layers

5. FUNDING NUMBERS

WU-505-90-5K

6. AUTHOR(S)

Thomas F. Balsa

7. PERFORMING ORGANIZATION NAME(S) AND ADDRESS(ES)

National Aeronautics and Space Administration
Lewis Research Center
Cleveland, Ohio 44135-3191

8. PERFORMING ORGANIZATION REPORT NUMBER

E-9218

9. SPONSORING/MONITORING AGENCY NAME(S) AND ADDRESS(ES)

National Aeronautics and Space Administration
Washington, D.C. 20546-0001

10. SPONSORING/MONITORING AGENCY REPORT NUMBER

NASA TM-106770
ICOMP-94-26

11. SUPPLEMENTARY NOTES

Thomas F. Balsa, Institute for Computational Mechanics in Propulsion, NASA Lewis Research Center (work funded under NASA Cooperative Agreement NCC3-233), and University of Arizona, Department of Aerospace and Mechanical Engineering, Tucson, Arizona 85721. ICOMP Program Director, Louis A. Povinelli, organization code 2600, (216) 433-5818.

12a. DISTRIBUTION/AVAILABILITY STATEMENT

Unclassified - Unlimited
Subject Category 34

12b. DISTRIBUTION CODE

13. ABSTRACT ***(Maximum 200 words)***

We consider analytically the evolution of a three-dimensional wave packet generated by an impulsive source in a mixing layer. The base flow is assumed to be spreading due to viscous diffusion. The analysis is restricted to small disturbances (linearized theory). A suitable high-frequency ansatz is used to describe the packet; the key elements of this description are a complex phase and a wave action density. It is found that the product of this density and an infinitesimal material volume convecting at the local group velocity is *not* conserved: there is a continuous interaction between the base flow and the wave action. This interaction is determined by suitable mode-weighted averages of the second and fourth derivatives of the base-flow velocity profile. Although there is some tendency for the dominant wavenumber in the packet to shift from the most unstable value toward the neutral value, this shift is quite moderate. In practice, wave packets do not become locally neutral in a diverging base flow (as do instability modes), therefore, they are expected to grow more suddenly than pure instability modes and do not develop critical layers. The group velocity is complex; the full significance of this is realized by analytically continuing the equations for the phase and wave action into a complex domain. The implications of this analytic continuation are discussed vis-a-vis the secondary instabilities of the packet: very small-scale perturbations on the phase can grow very rapidly initially, but saturate later because most of the energy in these perturbations is convected away by the group velocity. This remark, as well as the one regarding critical layers, has consequences for the nonlinear theories.

14. SUBJECT TERMS

Mixing layers; Wave packets; Unstable shear flows

15. NUMBER OF PAGES 49

16. PRICE CODE A03

17. SECURITY CLASSIFICATION OF REPORT	18. SECURITY CLASSIFICATION OF THIS PAGE	19. SECURITY CLASSIFICATION OF ABSTRACT	20. LIMITATION OF ABSTRACT
Unclassified	Unclassified	Unclassified	

NSN 7540-01-280-5500

Standard Form 298 (Rev. 2-89)
Prescribed by ANSI Std. Z39-18
298-102